Vascular endothelial adrenomedullin-RAMP2 system is essential for vascular integrity and organ homeostasis

Teruhide Koyama[1,6], Laura Ochoa-Callejero Ph.D.[2], Takayuki Sakurai Ph.D.[1], Akiko Kamiyoshi Ph.D.[1], Yuka Ichikawa-Shindo M.D., Ph.D.[1], Nobuyoshi Iinuma M.D., Ph.D.[1], Takuma Arai M.D., Ph.D.[1], Takahiro Yoshizawa[1,6], Yasuhiro Iesato M.D.[1], Yang Lei[1], Ryuichi Uetake[1], Ayano Okimura[1], Akihiro Yamauchi[1], Megumu Tanaka[1], Kyoko Igarashi[1], Yuichi Toriyama M.D.[1], Hisaka Kawate[1], Ralf H. Adams Ph.D.[3], Hayato Kawakami M.D., Ph.D.[4], Naoki Mochizuki M.D., Ph.D.[5], Alfredo Martínez Ph.D.[2], Takayuki Shindo M.D., Ph.D.[1]

[1] Department of Cardiovascular Research, Shinshu University Graduate School of Medicine
[2] Oncology Area, Center for Biomedical Research of La Rioja
[3] Department of Tissue Morphogenesis, University of Munster
[4] Department of Anatomy, Kyorin University School of Medicine
[5] Department of Structural Analysis, National Cardiovascular Center Research Institute
[6] Research Fellow of the Japan Society for the Promotion of Science

Short title : Adrenomedullin-RAMP2 system in vascular integrity
Word Count: 6,950
Subject Code:
[130] Animal models of human disease, [129] Angiogenesis, [134] Pathophysiology, [145] Genetically altered mice, [95] Endothelium/vascular type/nitric oxide

Address for correspondence
Takayuki Shindo, MD, PhD
Department of Cardiovascular Research
Shinshu University Graduate School of Medicine
Asahi 3-1-1, Matsumoto, Nagano, 390-8621, Japan
Tel: +81-263-37-3192
Fax: +81-263-37-3437
Email: tshindo@shinshu-u.ac.jp

Abstract

Background- Revealing the mechanisms underlying the functional integrity of the vascular system could make available novel therapeutic approaches. We previously showed that knocking out the widely expressed peptide adrenomedullin (AM) or receptor activity-modifying protein 2 (RAMP2), an AM-receptor accessory protein, causes vascular abnormalities and is embryonically lethal. Our aim was to investigate the function of the vascular AM-RAMP2 system directly.

Methods and Results- We generated endothelial cell-specific RAMP2 and AM knockout mice (E-RAMP2-/-, E-AM-/-). Most E-RAMP2-/- mice died perinatally. In surviving adults vasculitis occurred spontaneously. With aging, E-RAMP2-/- mice showed severe organ fibrosis with marked oxidative stress and accelerated vascular senescence. Later, liver cirrhosis, cardiac fibrosis and hydronephrosis developed. We next used a line of drug-inducible E-RAMP2-/- mice (DI-E-RAMP2-/-) to induce RAMP2-deletion in adults, which enabled us to analyze the initial causes of the aforementioned vascular and organ damage. Early after the induction, pronounced edema with enhanced vascular leakage occurred. *In vitro* analysis revealed the vascular leakage to be caused by actin disarrangement and detachment of endothelial cells. We found that the AM-RAMP2 system regulates the Rac1-GTP/RhoA-GTP ratio and cortical actin formation, and that a defect in this system causes the disruption of actin formation, leading to vascular and organ damage at the chronic stage after the gene deletion.

Conclusions- Our findings show that the AM-RAMP2 system is a key determinant of vascular integrity and homeostasis from prenatal stages through adulthood. Furthermore, our

models demonstrate how endothelial cells regulate vascular integrity and how their dysregulation leads to organ damage.

Key Words:

arteriosclerosis

vasculature

endothelium

edema

aging

Non-standard Abbreviations

AM: Adrenomedullin

RAMP: Receptor activity-modifying protein

CLR: Calcitonin-receptor-like receptor

DI-E-: Drug-inducible endothelial cell specific-

LSEC: Liver sinusoidal endothelial cell

Potential clinical impact of our paper

Adrenomedullin (AM), originally identified as a vasodilating peptide, is now recognized to be a pleiotropic vasoactive molecule involved in both the pathogenesis of cardiovascular diseases and circulatory homeostasis. Because of its wide range of bioactivity, AM has been attracting a lot of attention for its potential clinical applications. On the other hand, the clinical applicability of AM, like that of other bioactive endogenous peptides, has limitations: AM has a very short half-life in the blood, which makes the use of AM impractical for the treatment of chronic diseases. It is noteworthy that we were able to modulate the vascular function of AM by modulating RAMP2. RAMP2 in particular could be a therapeutic target via which to manipulate the vascular functions of AM. Because RAMPs are low molecular weight proteins, structural analysis and the synthesis of specific agonists or antagonists are much more realistic compared with the AM receptor CLR, which belongs to seven-transmembrane domain G protein-coupled receptors (GPCRs). The vascular AM-RAMP2 system plays critical roles in the regulation of vascular integrity, including the maintenance of vascular structure, regulation of angiogenesis, and vasoprotection against vascular injury. In that context, studies of AM and RAMP2 should bring about novel approaches for the treatment of diseases derived from vascular failure. Conditional gene targeting models in this study, which enable the spatial and temporal modulation of the gene expression, could elucidate the detailed pathophysiological roles of the AM-RAMP2 system.

Introduction

Chronic organ dysfunction is the most common cause of morbidity among aging individuals. Generally, the process of organ dysfunction begins slowly, but it is progressive and intractable in its chronic phase. From a mechanistic viewpoint, chronic organ dysfunction can be explained as a disruption of physiological homeostasis and the processes responsible for organ maintenance and repair. This is particularly true for the vascular system, which plays central roles in the maintenance of organ homeostasis[1, 2]. Revealing the mechanisms underlying the functional integrity of the vascular system could make available novel therapeutic approaches to the treatment of organ dysfunction.

Vascular endothelial cells (ECs) and vasoactive molecules play key roles in the maintenance of vascular homeostasis[3, 4]. ECs actively secrete a variety of bioactive molecules, including nitric oxide, atrial natriuretic peptide (ANP), prostacyclin and adrenomedullin (AM). Originally identified as a vasodilating peptide isolated from human pheochromocytoma[5], AM is now known to be widely secreted from a variety of organs and tissues, including ECs, and to be involved in a number of biological functions[6–13]. Plasma levels of AM are elevated in patients with such cardiovascular diseases as hypertension and congestive heart failure[14, 15]. Moreover, it was recently reported that plasma AM levels are a highly sensitive marker of chronic kidney disease (CKD) that may be predictive of its prognosis[16]. We previously showed that homozygotic AM knockout (KO) (AM-/-) mice die at mid-gestation due to edema and hemorrhage, and clarified the critical role of AM in angiogenesis[17]. Heterozygotic AM KO (AM+/-) mice grow to adulthood with no apparent deficits, but show accelerated cardiac hypertrophy, fibrosis, renal failure, and arteriosclerosis

upon cardiovascular injury. Given these observations, the clinical application of AM has been much anticipated[18-22]; however, AM is a peptide with a short half-life in the bloodstream, which limits its usefulness for the treatment of chronic diseases.

To overcome that limitation, we have been focusing on AM's receptor system. AM is a member of the calcitonin superfamily and acts via a G protein-coupled seven transmembrane domain receptor, calcitonin-receptor-like receptor (CLR)[23, 24]. The specificity of CLR for its ligands is regulated by a group of three receptor-activity-modifying proteins, RAMP1, -2 and -3. We have shown that homozygotic RAMP2 KO (RAMP2-/-) mice die in utero. Interestingly, among the RAMP KO mice, RAMP2-/- mice die from vascular abnormalities similar to those observed in AM-/- mice[25]. This suggests RAMP2 is the key determinant of AM's vascular function.

Our aim in the present study was to clarify the pathophysiological function of the vascular AM-RAMP2 system directly. To accomplish that, we generated and utilized four KO models: EC-specific (E)-RAMP2-/-, aged conventional RAMP2+/-, drug-inducible (DI)-E-RAMP2-/- and EC-specific (E)-AM-/- mice. With these models, we were able to determine both the acute and chronic effects of RAMP2 deletion, and demonstrate the contribution made by the AM-RAMP2 system to the maintenance of vascular integrity and organ homeostasis.

Methods

Mouse models

Vascular endothelial cadherin (VE-cadherin) Cre transgenic mice and mice expressing tamoxifen-inducible Cre-recombinase (Cre-ERT2) under the regulation of VE-cadherin promoter were crossed with floxed RAMP2 mice (RAMP2flox/flox) to create vascular EC-specific RAMP2 conditional KO mice (E- RAMP2-/-) (Fig. 1a) and tamoxifen drug-inducible (DI) vascular EC-specific RAMP2 KO mice (DI-E-RAMP2-/-) (Fig. 6a), respectively.

Quantitative real-time RT-PCR analysis

The primers and probes used are listed in Supplemental Table. 3.

For other experimental procedures, please refer to Supplemental File.

Results

Generation of vascular EC-specific RAMP2 KO mice

Conventional RAMP2-/- embryos died at mid-gestation (around 14.5 dpc), as we reported previously[25]. By contrast, EC-specific RAMP2-/- (E-RAMP2-/-) embryos survived until later in development, though most died during the perinatal period (Fig. 1b). Among the $RAMP2^{flox/flox}$ Cre+/- intercrosses, the estimated survival rate of E-RAMP2-/- mice at 4 weeks of age was less than 5% (Supplemental Table 1). Perinatal stage E-RAMP2-/- mice exhibited systemic edema (Fig. 1c, d), as well as interstitial edema within the intestinal villi (Fig. 1e) and lung (Fig. 1f), and severe hemorrhagic changes within the liver (Fig. 1g). As expected, E-RAMP2-/- mice showed vascular abnormalities, including malformation of aortic ECs (Fig.1h) and partial detachment of ECs from the basement membrane (Fig.1i, j).

Abnormalities in the vascular structure of surviving E-RAMP2-/- adults

In the 5% of E-RAMP2-/- mice that survived until adulthood, RAMP2 expression in aortic ECs was 20% of that in their littermate controls (Cont) (data not shown). The surviving E-RAMP2-/- adults also exhibited thinning of the aortic wall and enlarged aortic diameters (Fig. 1k, l). Both systolic and diastolic blood pressures (SBP and DBP) were lower in E-RAMP2-/- than Cont mice (Fig. 1m). Electron microscopic observation revealed that the aortic smooth muscle layer was in disarray in E-RAMP2-/- mice (Fig. 1o), and that the ECs were detached from the basement membrane and severely deformed (Fig. 1n). These morphological changes in the vascular cells may partially explain the enlargement of the aorta and reduction in blood pressure. Given these observations, we speculated that EC

viability was diminished in E-RAMP2-/- mice, which was confirmed by the severe disruption of angiogenesis seen in *ex vivo* aortic ring assays (Fig. 1p).

Severe vascular inflammation and organ fibrosis in E-RAMP2-/- adults

Vasculitic lesions developed spontaneously in surviving E-RAMP2-/- adults, beginning when they were about 6-month-old, and severe infiltration and accumulation of inflammatory cells was observed in blood vessels within the major organs, including the liver (Fig. 2a), kidneys (Fig. 2b) and lungs (Fig. 2c). The infiltrating cells were CD3+ or F4/80+, which is indicative of T cells and macrophages, respectively (Fig. 2d, e). In addition, the expression of inflammatory cytokines and macrophage markers was also upregulated (Fig. 2f).

We speculated that the vascular damage in the surviving adult E-RAMP2-/- mice was the primary cause of the vasculitis. In that regard, it was recently suggested that vascular damage may be the cause of vascular senescence[26, 27]. To test whether these phenomena indicate accelerated senescence, we next evaluated aged conventional RAMP2 KO mice (RAMP2+/-). At 2 years of age, RAMP2+/- mice showed inflammatory cell infiltration of the main organs (Fig. 2g-i). Senescence-associated (SA)-β-gal staining, which is commonly used to assess accelerated aging, was more intense in the aortas of the aged RAMP2+/- than WT mice (Fig. 2j). Moreover, the SA-β-gal staining could be detected at a much younger age (6 months) in E-RAMP2-/- mice (Fig. 2k).

The presence of activated Akt and p53 in the aorta is another recognized marker of vascular senescence[28]. Levels of Akt and p53 activation were much greater in aged RAMP2+/- than WT mice (Fig. 2l). No difference was seen between the levels of Akt and p53 activation in younger RAMP2+/- and WT mice, though the inflammatory cell adhesion

markers ICAM-1 and VCAM-1 were already upregulated in the young RAMP2+/- animals. This is consistent with the idea that vascular senescence is preceded by vascular damage and inflammation.

More interestingly, organ damage developed spontaneously in E-RAMP2-/- adults. In particular, the livers of E-RAMP2-/- mice appeared cirrhotic by the time the animals were 6 months old (Fig. 3a). Pathological analysis revealed that the cirrhosis-like changes were not caused by damage to parenchymal hepatocytes, but by severe fibrosis along the vasculature within the liver, most likely due to dysfunction of the sinusoidal ECs (Fig. 3b, c). Cardiac enlargement with interstitial fibrosis was also seen in 6-month-old E-RAMP2-/- mice (Fig. 3d, e). In addition, quantitative real-time PCR showed elevated expression of ANP, brain natriuretic peptide (BNP) and transforming growth factor-β (TGF-β), which is indicative of heart failure and fibrosis (Fig. 3f). In addition, spontaneous hydronephrosis (Fig. 3g) and polycystic changes (Fig. 3h) were noted in the kidneys of E-RAMP2-/- mice, as was glomerular enlargement and sclerotic changes (Fig. 3i). Electron microscopy revealed podocyte fusion, hyperplasia of the basal membrane, and partial dehiscence between the glomerular ECs and basal membrane (Fig. 3j). Renal expression of TGF-β and collagen was also upregulated in E-RAMP2-/- mice (Fig. 3k).

EC-specific AM KO mice showed vascular inflammation and glomerulosclerosis

We next compared EC-specific AM KO (E-AM-/-) with E-RAMP2-/-. In contrast to E-RAMP2-/- neonates, E-AM-/- neonates were healthy and presented no overtly pathophysiological phenotypes (Supplemental Table 2). We suggest that in E-AM-/- neonates, circulating and/or paracrine AM from sources other than ECs likely attenuate the

phenotypes observed in E-RAMP2-/- neonates. In adults, however, the vascular inflammation and organ damage were similar to those seen in E-RAMP2-/- mice. E-AM-/- mice showed severe infiltration and accumulation of inflammatory cells around the vasculature (Fig. 4a, b). They also showed glomerulosclerotic changes with mesangial expansion and upregulation of inflammatory molecules (Fig. 4c-e).

RAMP2 deficiency enhances inflammatory reactions in both ECs and leukocytes

We speculated that the observed vasculitic lesions began with the cellular adhesion of inflammatory cells to ECs. To test that idea, we initially examined the effect of endothelial RAMP2-deficiency on the interaction between ECs and macrophages *in vitro*. After isolating and culturing LSECs from RAMP2+/- and WT mice, we evaluated the attachment of macrophages isolated from GFP-mice (provided by Prof. Sato of Kagoshima University). We found that GFP+ macrophages attached more readily to RAMP2+/- LSECs than to WT LSECs (Fig. 5a, b), and that VCAM-1 expression was higher in RAMP2+/- LSECs than in WT cells (Fig. 5c).

To then assess the effect of RAMP2-deficiency on the leukocytes, we crossbred DsRed+ (provided by Dr. Tagawa of the Tokyo Institute of Technology) with RAMP2+/- mice to generate a DsRed+RAMP2+/- mouse line. We found that both peripheral leukocytes (Fig. 5d, e) and peritoneal macrophages (Fig. 5f, g) collected from DsRed+RAMP2+/- attached more readily to LSECs than did WT. Phagocytosis of macrophages was not different between WT and RAMP2+/- (Fig. 5h, i), however, expression of the inflammation markers, including monocyte chemotactic protein-1 (MCP-1), interleukin-6 (IL-6), and IL-1β were upregulated in RAMP2+/- macrophages (Fig. 5j). This suggests that

attached more readily to LSECs than did WT. Phagocytosis of macrophages was not different between WT and RAMP2+/- (Fig. 5h, i), however, expression of the inflammation markers, including monocyte chemotactic protein-1 (MCP-1), interleukin-6 (IL-6), and IL-1β were upregulated in RAMP2+/- macrophages (Fig. 5j). This suggests that RAMP2-deficiency in leukocytes, as well as in ECs, enhances inflammatory reactions, and that both likely contribute to the chronic inflammation observed in aged RAMP2+/- mice.

RAMP2 deficiency increases oxidative stress, while RAMP2 overexpression leads to resistance to senescence under conditions of oxidative stress in ECs

It has been reported that AM exerts antioxidant effects. In 6-month-old E-RAMP2-/- mice, we detected elevated levels of oxidative stress in the major organs. Levels of 4-hydroxy-2-nonenal (4HNE) immunostaining, which reveals the presence of peroxides of unsaturated fatty acids, were increased in E-RAMP2-/- (Fig. 5k). Consistent with this finding, expression of three NADPH-oxidase subunits (p22-phox, p47-phox and p67-phox) were elevated (Fig. 5l). Thus RAMP2-deficiency in ECs appears to exacerbate oxidative stress.

We next used EAhy926 ECs to generate EC lines stably overexpressing RAMP2. H_2O_2-treatment has been shown to induce EC senescence[29]. We found that after incubation for 24 h in the presence of H_2O_2 plus AM, control cells were strongly stained by SA-β-gal, but cells overexpressing RAMP2 were resistant to staining (Fig. 5m).

Initial EC change elicited by RAMP2 deletion in drug-inducible EC-specific RAMP2 KO mice

As mentioned, most E-RAMP2-/- mice died as neonates and analysis using adult mice

d). The cause of the edema was enhanced vascular permeability and plasma leakage, as evidenced by the extravascular leakage of Evans Blue dye (Fig. 6e). In a hind-limb ischemia model, which enables us to evaluate the post-natal angiogenic potency, we also found that blood flow recovery was delayed in DI-E-RAMP2-/- (Fig. 6f).

Next, we evaluated whether we could rescue the phenotype of DI-E-RAMP2-/- by vascular overexpression of RAMP2 gene. We employed the gene delivery method in the hind-limb ischemia model by electroporation of plasmid, which could overexpress RAMP2 under the control of VE-cadherin promoter (Supplemental Fig. 1). At first, we confirmed the VE-cadherin promoter works only in vascular endothelial cells; when VE-cadherin-EGFP plasmid is electroporated at the femoral region, the signal was detected only at the isolectin-positive endothelial cells (Fig. 6g). In addition, after 24 h of electroporation of VE-cadherin-RAMP2 plasmid, we confirmed that RAMP2 expression was strongly induced in DI-E-RAMP2-/- (Fig. 6h). Actually, the RAMP2 gene delivery in DI-E-RAMP2-/- successfully restored the blood flow recovery in the hind-limb ischemia (Fig. 6i, j). Moreover, the RAMP2 gene delivery enhanced capillary formation and reduced interstitial edema in DI-E-RAMP2-/- (Fig. 6k, l).

Using the DI-E-RAMP2-/- line, we further evaluated the primary cause of the vascular failure. In electron micrographs of aortas obtained 2 weeks after RAMP2-deletion, ECs in DI-E-RAMP2-/- mice appeared deformed and were detached from the basement membrane (Fig. 6m). We speculated that the cause was cytoskeletal abnormality within the ECs. Consistent with that idea, actin polymerization in DI-E-RAMP2-/- ECs appeared in disarray, and there was a loss of actin-bundle formation under the plasma membrane (cortical actin formation) (Fig. 6n). It has been reported that small GTPases, Rac1 and RhoA, play crucial

roles in the regulation of ECs' barrier function by regulating the formation cortical actin and stress fibers[30]. When we analyzed the activation of Rac1 and RhoA in DI-E-RAMP2-/- ECs, we found that levels of the activated form of Rac1 (Rac1-GTP) were significantly reduced, whereas the activated form of RhoA (RhoA-GTP) was increased (Fig. 6o, p). On the other hand, AM-treatment enhanced cortical actin formation in HUVECs (Fig. 6q). Notably, the Rac1 inhibitor NSC23766 blocked the AM-induced enhancement of cortical action formation, whereas Rho-associated protein kinase (ROCK) inhibitor Y27632 had no effect (Fig. 6r). Taken together, these observations suggest the AM-RAMP2 system regulates the Rac1-GTP/RhoA-GTP ratio and therefore cortical actin formation, and that a defect in this system will disrupt actin formation.

We also confirmed that at the chronic stage after the gene-deletion, DI-E-RAMP2-/- mice exhibited vascular damage with enhanced perivascular inflammation that was the same as that of adult E-RAMP2-/- (Fig. 7). With DI-E-RAMP2-/-, therefore, we were able to clarify both the acute and chronic effects of RAMP2 deletion in the adult, and demonstrate that RAMP2 is essential for EC viability, vascular integrity, and homeostasis.

Discussion

Our initial finding was that most E-RAMP2-/- mice die perinatally from severe systemic edema. In contrast to conventional RAMP2-/- embryos, which die at mid-gestation, E-RAMP2-/- embryos survived until later stages of development. As we and other groups reported previously, in conventional RAMP2-/- embryos, deformity was detected in both the endothelium and the smooth muscle layer in both blood and lymphatic vessels[25, 31]. By contrast, in the E-RAMP2-/- embryos used in this study, the lesion was limited in the ECs, which likely accounts for their longer survival. Nonetheless, most E-RAMP2-/- died due to edema, reflecting the endothelial abnormality and vascular leakage. Clearly, endogenous RAMP2 is essential for EC viability and vascular integrity.

About 5% of E-RAMP2-/- mice survived to adulthood. E-RAMP2-/- adults were apparently normal when young, but showed EC deformity and reduced viability later. Interestingly, the cellular deformities in the adult animals was not limited to the endothelium, but also included the smooth muscle cell layer, which suggests the congenital EC abnormalities induced secondary postnatal disorder of other vascular component cells. E-RAMP2-/- mice also had lower blood pressures than WT mice, which seems contradictory, as AM is well known to be a vasodilator. We speculate that the reduction in blood pressure might be due to the observed morphological changes in the vascular cells. Another possibility is that our findings are consistent with the report that although AM is a vasodilator when injected peripherally, it is a vasoconstrictor when injected intracerebrally[32]; that is, when endothelial RAMP2 deficiency affects both peripheral and central AM signaling, the expected central phenotype is observed.

E-RAMP2-/- adults also showed marked accumulation of inflammatory cells along the blood vessels within major organs, and the chronic vascular damage by such inflammation can accelerate vascular senescence[28, 33-35]. We found that activation of aortic Akt and p53, as well as SA-β-gal staining, two indicators of vascular senescence, were enhanced in adult E-RAMP2-/- mice, and that similar vasculitic lesions were present in aged conventional RAMP2+/- mice. The vascular lesions in E-RAMP2-/- mice led to organ damage, which included liver cirrhosis, cardiac enlargement with fibrosis, hydronephrosis, polycystic changes in the kidney and glomerulosclerosis. Taken together, these findings suggest that endothelial RAMP2 deficiency is the primary cause of subsequent vascular inflammation, accelerated senescence, fibrosis, and chronic organ dysfunction.

Unlike virus-related liver cirrhosis, in which the lesion starts within the hepatocytes, the cirrhotic changes seen in E-RAMP2-/- mice were caused by severe fibrosis that started in the vasculature. This is consistent with idea that vascular damage is the primary cause of this cirrhosis. In the E-RAMP2-/- kidney, both glomerular and interstitial changes were observed, along with epithelial cell damage (podocyte fusion) associated with glomerular EC deformity. And in the heart, cardiac enlargement and fibrosis led to heart failure. Thus loss of EC viability and vascular integrity accelerated vascular senescence and exacerbated interstitial lesions, making it the primary cause of chronic organ dysfunction.

For this study, we also generated EC-specific AM KO mice (E-AM-/-). In contrast to E-RAMP2-/- neonates, the E-AM-/- neonates appeared healthy. It seems the phenotype caused by knocking out the ligand during development is much milder than the one caused by knocking out the receptor. This is likely because AM is secreted from cells other than ECs, and circulating and/or paracrine AM from these other sources compensate for the endothelial

AM deficiency during development. In adults, however, the chronic reduction in AM signaling led to vascular inflammation and chronic organ damage in E-AM-/- mice, suggesting that aging is another important factor contributing to the emergence of the pathophysiological phenotype.

To better understand the mechanism by which endothelial RAMP2 deficiency could promote the aforementioned pathological features, we first characterized the inflammatory response triggered in RAMP2-deficient ECs. We recently reported that the expression of adhesion markers was downregulated by AM[36]. In the absence of AM signaling in RAMP2-deficient ECs in the present study, these inflammatory adhesion molecules were upregulated, facilitating the attachment of macrophages. This inflammatory response, along with the partial detachment of ECs from the basement membrane, likely accelerates the attachment, transmigration and accumulation of inflammatory cells within the vascular wall.

We also found high levels of oxidative stress, including elevation of NADPH-oxidase levels, within the major organs of E-RAMP2-/- mice. It has been reported that AM exerts strong antioxidant effects[9], and in the present study AM protected ECs stably overexpressing RAMP2 from cellular senescence induced by oxidative stress. This suggests that AM-RAMP2 signaling suppresses oxidative stress, and that endothelial RAMP2 may be an effective target through which to regulate oxidative stress.

Because most E-RAMP2-/- mice die as neonates, analysis of adult animals has been limited. To overcome this limitation, we generated a drug-inducible EC-specific RAMP2 KO mouse (DI-E-RAMP2-/-). In this model, we can induce RAMP2 gene deletion in adults on demand and then analyze the changes induced by RAMP2 deletion. Interestingly, DI-E-RAMP2-/- mice exhibit marked systemic edema caused by increased vascular

permeability. It is widely recognized that an increase in intracellular cyclic adenosine monophosphate (cAMP) within ECs strengthens their barrier function and reduces endothelial permeability, both in vitro and in vivo[30, 37]. It is therefore not surprising that cAMP-elevating G protein-coupled receptor agonists, such as AM, prostacyclin and prostaglandin E2, reduce endothelial hyperpermeability induced by inflammatory stimuli[38]. In addition, small GTPases, especially Rac1 and RhoA, play crucial roles in the regulation of EC barrier function by regulating the formation of cortical actin and stress fibers, respectively[30]. Elevation of cAMP leads to Rac1 activation, which in turn strengthens endothelial barrier function by enhancing cortical actin ring formation[39]. We found that in DI-E-RAMP2-/- ECs, actin polymerization was disrupted and Rac1 activation was reduced. By contrast, AM-stimulated ECs showed cortical actin formation, which disappeared upon treatment with a Rac1 inhibitor. Taken together, these findings suggest that in DI-E-RAMP2-/- ECs, downregulation of cAMP production and Rac1 activation reduces cortical actin formation, diminishing endothelial barrier function.

The relationship between the AM receptor and human disease has also been reported. A human SNP study described the relationship between CLR with essential hypertension[40]. A human study also revealed the relationship between RAMP1 SNPs with the incidence of cerebral infarction [41]. Some human mutations of RAMP3 gene have also been reported [42]. On the other hand, there have been no reports on human RAMP2 gene mutation. As we have shown, RAMP2-deletion can cause embryonic lethality at mid-gestation, and this may be one reason that we cannot see human congenital disease. In this context, the endothelial cell-specific conditional knockout mice model in this study should be recognized as a model of vascular failure and relevant organ dysfunction and should not be recognized as a specific

congenital disease model.

In this study, we were able to clarify both the acute and chronic effects of RAMP2 deletion in the adult, and to demonstrate that the AM-RAMP2 system is essential for vascular integrity and organ homeostasis. The illustration in Figure 8 summarizes the series of phenomena stemming from RAMP2 deletion. Early after RAMP2 gene deletion, ECs show morphological changes due to actin filament abnormality (disappearance of the cortical actin ring and disarray of actin polymerization). The resultant EC deformation causes detachment, barrier dysfunction, enhanced vascular permeability and edema, which in turn promote the attachment and infiltration of inflammatory cells. Chronic vascular inflammation induces vascular damage and accelerated senescence, and enhances oxidative stress and organ fibrosis. Finally, the accumulated disorders cause chronic organ dysfunction with aging. The results obtained using these models demonstrate that vascular EC integrity is essential for organ homeostasis. We also suggest that RAMP2, via which we could modulate vascular integrity, is a potentially useful therapeutic target for the treatment of chronic organ dysfunction.

Acknowledgement

The authors thank Dr. Sandra Hervás for her assistance with cell sorting.

Funding Sources

This study was supported by the Funding Program for Next Generation World-Leading Researchers (NEXT Program) from the Cabinet Office, Government of Japan and Innovation Grant from Spain´s Ministry of Science (SAF2009-13240-C02-01).

Disclosures

None

Figure legend

Fig. 1

E-RAMP2-/- mice showed systemic edema and high perinatal mortality, while surviving adult mice showed vascular abnormalities

(a) Strategy of conditional gene targeting of mouse RAMP2. A RAMP2 floxed mouse was crossbred with a VE-cadherin promoter-driven Cre recombinase-expressing mouse (lower panel) to generate vascular endothelial cell-specific RAMP2-/- mice (E-RAMP2-/-).

(b) E-RAMP2-/- survival curve. E-RAMP2-/- embryos generally survived at least until the perinatal period.

(c, d) E19.5 E-RAMP2-/- embryos showed systemic edema (**c**) with increased body weight (**d**). n = 11 in both Control and E-RAMP2-/-. Bars are means ± SEM. **p<0.01

(e-g) H&E staining of the intestine (**e**), lung (**f**) and liver (**g**) from E19.5 $RAMP2^{flox/flox}$ mice (Cont) and E-RAMP2-/-. Scale bars = 50μm (**e**), 400μm (**f**), and 200μm (**g**)

(h-j) Electron micrographs of aortas from E19.5 Cont and E-RAMP2-/-. E-RAMP2-/- ECs were detached (arrows). Scale bars = 5μm.

(k, l) H&E staining of aortas from adult Cont and E-RAMP2-/-. Scale bars = 300μm (**k**), 50 μm (**l**).

(m) Blood pressures in adult Control and E-RAMP2-/- mice. SBP systolic blood pressure; DBP diastolic blood pressures. n = 12 in Control and n=9 in E-RAMP2-/-. Bars are means ± SEM. **p<0.01.

(n, o) Electron micrographs of adult aortas. E-RAMP2-/- aortas showed detachment of ECs (**n**) and a disordered smooth muscle layer (**o**). Scale bars = 5 μm.

(p) *ex vivo* analysis of angiogenesis using adult aortic ring specimens after 14 days of culture in collagen gel.

Fig. 2

Adult E-RAMP2-/- mice showed spontaneous vasculitic lesions and premature vascular senescence

(a-e) Severe infiltration and accumulation of inflammatory cells in blood vessels within major organs of adult E-RAMP2-/-. Histology (H&E staining) of liver (**a**), kidney (**b**) and lung (**c**) from Cont and E-RAMP2-/- is shown. E-RAMP2-/- showed spontaneous vascular lesions, beginning at about 6 months of age. Immunohistological analysis revealed these cells to be CD3+ (**d**) or F4/80+ (**e**), which is indicative of T cells and macrophages, respectively.

(f) Quantitative real-time PCR analysis of kidney showing upregulation of inflammatory cytokines and macrophage markers in E-RAMP2-/-. n = 6 in Control and n = 3 in E-RAMP2-/-. Bars are means. *$p<0.05$.

(g-i) Vasculitic lesions similar to those in E-RAMP2-/- were confirmed in aged (2-year-old) conventional RAMP2+/- (Scale bars = 100μm).

(j, k) SA-β-gal staining of aorta. In aged mice (2 year-old), aortic SA-β-gal staining was more intense in RAMP2+/- than wild-type mice (WT) (**j**). The SA-β-gal positivity was detected much earlier (6 months of age) in E-RAMP2-/- than Cont (**k**).

(l) Western blot analysis of aortas from RAMP2+/- and WT. p53 and Akt were more activated in aged (2-year-old) RAMP2+/- than WT (right panel), but not in younger (9-week-old) mice (left panel). However, expression of ICAM-1 and VCAM-1 was already

upregulated in young RAMP2+/- (left panel).

Fig. 3

E-RAMP2-/- mice showed fibrosis starting around vessels and progression of organ damage

(a) Livers appeared cirrhotic in 6-month-old E-RAMP2-/- mice.

(b, c) Silver (**b**) and sirius red (**c**) staining of E-RAMP2-/- livers showed severe fibrosis along the vasculature. Scale bars = 100μm.

(d, e) Cardiac enlargement with interstitial fibrosis in 6-month-old E-RAMP2-/- mice. Gross appearance (**d**) and histology (Masson trichrome staining) of the heart (**e**) are shown. Scale bars = 200μm.

(f) Quantitative real-time PCR analysis of hearts from Cont and E-RAMP2-/- mice. Expression of heart failure and fibrosis markers was upregulated in E-RAMP2-/- mice. n = 4 in both Control and E-RAMP2-/-. Bars are means ± SEM. **p<0.01.

(g-i) Histological abnormalities in the kidneys of E-RAMP2-/-. (**g**) Section of whole E-RAMP2-/- kidney showing an enlarged renal pelvis; (**h**) Section of renal cortex showing polycystic changes. Scale bars = 100 μm. (**i**) Enlargement of the glomerular area in a E-RAMP2-/- kidney. Scale bars = 50 μm. n = 4 in both Control and E-RAMP2-/-. Bars are means ± SEM. **p<0.01.

(j) Electron micrographs of glomeruli from Cont and E-RAMP2-/- kidneys. In the E-RAMP2-/- kidney, fusion of podocytes (upper panel) and detachment of ECs from the basement membrane (lower panel) are apparent (arrows). Scale bars = 1 μm.

(k) Quantitative real-time PCR analysis of Cont and E-RAMP2-/- kidneys. Fibrotic markers

were upregulated in E-RAMP2-/- kidneys. n = 4 in both Control and E-RAMP2-/-. Bars are means ± SEM. *p<0.05.

Fig. 4

Adult E-AM-/- mice showed spontaneous vasculitic lesions and glomerulosclerosis

(**a, b**) Vasculitic lesion showing accumulation of inflammatory cells in an aged (6-month-old) EC-specific AM-/- (E-AM-/-) mouse. Histology (H&E staining) of the liver from a Cont and E-AM-/- mouse is shown (**a**). The accumulated cells are CD3+ T cells (**b**). Scale bars = 100μm.

(c, d) Glomerulosclerotic changes in E-AM-/- kidneys. Sirius red staining shows excessive collagen deposits among mesangial cells and in a Bowman's capsule from an E-AM-/- kidney (**c**). Glomerular area was significantly enlarged in the E-AM-/- kidney **(d)**. Scale bars = 50 μm. n = 10 in both Control and E-AM-/-. Bars are means ± SEM. **p<0.01.

(e) Quantitative real-time PCR analysis showing upregulation of inflammatory and fibrosis markers in E-AM-/- kidneys. n = 10 in both Control and E-AM-/-. Bars are means ± SEM.

Fig. 5

RAMP2 deficiency enhances EC inflammatory reactions and oxidative stress

(a, b) Macrophage adhesion to ECs. Macrophage adhesion to LSECs cultured from WT or RAMP2+/- mice was analyzed. RAMP2+/- LSECs showed greater adhesion, which was indicated by a higher cell count. Scale bars = 100 μm. n = 8 in both WT and RAMP2+/-. Bars are means ± SEM. *p<0.05.

(c) Quantitative real-time PCR analysis of LSECs. n = 6 in both WT and RAMP2+/-. Bars

are means ± SEM. **p<0.01, *p<0.05.

(d-g) To analyze the effect of RAMP2 deficiency on peripheral leukocytes and macrophages, buffy coat and peritoneal macrophages collected from DsRed/RAMP2+/+ or DsRed/RAMP2+/- mice were cultured with LSECs from WT mice. Attached DsRed+ cells were photographed (**d, f**) and counted (**e, g**). RAMP2+/- leukocytes (**d, e**) and macrophages (**f, g**) showed greater attachment than those of WT. Scale bars = 100 μm. n = 8 in both WT and RAMP2+/-. Bars are means ± SEM. **p<0.01, ***p<0.001. (**h, i**) Effect of RAMP2 deficiency on phagocytosis of macrophages. Photographs (**h**) and dot plot (**i**) representing phagocytosis of FITC-labeled particles by macrophages (circles in the dot plot) are shown. Phagocytosis was not different between WT and RAMP2+/-. Scale bars = 50 μm. **(j)** Quantitative real-time PCR analysis of macrophages from RAMP2+/- and WT mice. n = 8 in both WT and RAMP2+/-. Bars are means ± SEM. **p<0.01.

(k) Enhanced oxidative stress in E-RAMP2-/- mice. Immunostaining of unsaturated fatty acid peroxides was enhanced in E-RAMP2-/- liver and kidney. Particularly strong staining was detected around central veins in the liver and renal tubules in the kidney. Scale bars = 200 μm.

(l) Quantitative real-time PCR analysis of NADPH-oxidase subunits in the kidney. n = 6 in Control and n = 3 in E-RAMP2-/-. Bars are means. *p<0.05.

(**m**) Suppression of oxidative stress-induced cellular senescence in ECs stably overexpressing (O/E) RAMP2. After 24 h of treatment with H_2O_2 (200 μmol/L) and AM (10^{-7} M), SA-β-gal positivity was detected in the control EAhy926 ECs, but not RAMP2-overexpressing cells. Scale bars = 100 μm.

Fig. 6

Analysis of vascular endothelial RAMP2 deficiency in adults using drug-inducible EC-specific RAMP2 KO mice (DI-E-RAMP2-/-)

(a) Strategy of drug-inducible conditional gene targeting of mouse RAMP2. A RAMP2 floxed mouse was crossbred with a VE-cadherin promoter-driven, tamoxifen-inducible Cre recombinase transgenic mouse to generate drug-inducible EC-specific RAMP2-/- mice (DI-E-RAMP2-/-).

(b) Quantitative real-time PCR analysis of LSECs cultured primarily from DI-E-RAMP2-/- mice (2 weeks after the treatment with tamoxifen or corn oil). In tamoxifen-treated mice, endothelial RAMP2 expression was reduced to about 20% of control, while AM expression was upregulated to 200% of control. n = 8 in both Control and DI-E-RAMP2-/-. Bars are means ± SEM. **p<0.01.

(c, d) Appearance and body weight changes after induction of RAMP2 deletion in adult (8-week-old) mice. After induction of RAMP2 deletion, the mice showed facial and systemic edema (**c**) and marked body weight gain (**d**). n = 8 in Control and n = 12 in DI-E-RAMP2-/-. Bars are means ± SEM. *p<0.05, **p<0.01.

(e) Photographs (back skin, ear, hindlimb) showing the extravascular leakage of Evans Blue dye after its intravenous injection. DI-E-RAMP2-/- mice showed much greater vascular leakage.

(**f**) Blood flow ratio obtained from laser Doppler analysis in unilateral hind-limb ischemia model of control and DI-E-RAMP2-/- mice. n = 7 in both Control and DI-E-RAMP2-/-. Bars are means ± SEM. *p<0.05, **p<0.01.

(**g**) Section of the femoral muscle electroporated with VE-cadherin-EGFP plasmid.

EGFP-signaling and red fluorescence of isolectin-staining are shown. Scale bars = 50 μm

(**h**) Quantitative real-time PCR analysis of RAMP2-expression in the femoral muscle of control and DI-E-RAMP2-/- mice electroporated with the indicated plasmids. n = 4 in each group. Bars are means ± SEM. *p<0.05 vs. control mice + control plasmid, †† p < 0.01 vs. DI-E-RAMP2-/- mice + control plasmid.

(i-l) Unilateral hind-limb ischemia model used to evaluate angiogenic potency by electroporation of the indicated plasmids. (**i**) Laser Doppler imaging. **(j)** Blood flow ratio of ischemic limb/control limb. n = 7-8 in each group. Bars are means ± SEM. **p<0.01 vs. control mice + control plasmid, †† p < 0.01 vs. DI-E-RAMP2-/- mice + control plasmid. **(k)** Sections showing the neovascularization (isolectin staining) and interstitial edema (H&E staining) of the femoral muscle. Scale bars = 100 μm. **(l)** Bar graphs showing the capillary density and interstitial edema area quantified from each section. n = 4-5 in each group. Bars are means ± SEM. *p<0.05, **p<0.01 vs. control mice + control plasmid, †† p < 0.01 vs. DI-E-RAMP2-/- mice + control plasmid. **(m)** Electron micrographs of aortas obtained 2 weeks after gene deletion. DI-E-RAMP2-/- vessels showed detachment of ECs (arrows). Scale bars = 1 μm.

(n) LSECs cultured from control and DI-E-RAMP2-/- mice were stained with rhodamine-phalloidin to visualize F-actin. Scale bars = 50 μm.

(o) Western blots of Rac1-GTP, total Rac1, Rho-GTP and total Rho from ECs.

(**p**) Densitometric analysis of the Western blots. n = 3 in both Control and DI-E-RAMP2-/-. Data are show as the relative ratio to Control. Bars are means. *p<0.05.

(q) Effect of AM on HUVECs. HUVECs were stained with rhodamine-phalloidin to visualize F-actin. The cell in the right panel was stimulated for 30 min with 10^{-7} M AM.

Scale bars = 50 μm.

(r) Effect of AM with and without a Rho kinase or Rac1 inhibitor on mouse LSECs. Mouse LSECs were treated for 180 min with 10^{-7} M AM with and without10^{-4} M NSC23766 (Rac1 inhibitor) or 10^{-5} M Y27632 (ROCK inhibitor). Scale bars = 50 μm.

Fig. 7

Chronic RAMP2-deficiency causes vascular damage and enhanced perivascular inflammation in DI-E-RAMP2-/- mice

(a-c) Histology (H&E staining) of liver **(a)**, kidney **(b)** and lung **(c)** collected at the chronic stage. Severe infiltration and accumulation of inflammatory cells around blood vessels was detected in DI-E-RAMP2-/- mice but not in the control mice (Cont). Scale bars =100 μm.

Fig. 8

Regulation of EC integrity by the AM-RAMP2 system and its disruption in RAMP2 KO mice

The AM-RAMP2 system regulates cortical actin formation in ECs and barrier integrity through upregulation of cAMP and activation of Rac1. RAMP2 deletion disrupts actin polymerization in ECs and causes barrier dysfunction, which in turn leads to enhanced vascular permeability, infiltration of inflammatory cells, vascular damage and accelerated vascular senescence. These accumulated disorders cause chronic organ dysfunction with aging.

References

1. Cleaver O, Melton DA. Endothelial signaling during development. *Nat Med*. 2003;9:661-668
2. Carmeliet P. Angiogenesis in health and disease. *Nat Med*. 2003;9:653-660
3. Ross R. Atherosclerosis--an inflammatory disease. *N Engl J Med*. 1999;340:115-126
4. Higashi Y, Noma K, Yoshizumi M, Kihara Y. Endothelial function and oxidative stress in cardiovascular diseases. *Circ J*. 2009;73:411-418
5. Kitamura K, Kangawa K, Kawamoto M, Ichiki Y, Nakamura S, Matsuo H, Eto T. Adrenomedullin: A novel hypotensive peptide isolated from human pheochromocytoma. *Biochem Biophys Res Commun*. 1993;192:553-560
6. Abe M, Sata M, Nishimatsu H, Nagata D, Suzuki E, Terauchi Y, Kadowaki T, Minamino N, Kangawa K, Matsuo H, Hirata Y, Nagai R. Adrenomedullin augments collateral development in response to acute ischemia. *Biochemical and biophysical research communications*. 2003;306:10-15
7. Kato K, Yin H, Agata J, Yoshida H, Chao L, Chao J. Adrenomedullin gene delivery attenuates myocardial infarction and apoptosis after ischemia and reperfusion. *American journal of physiology. Heart and circulatory physiology*. 2003;285:H1506-1514
8. Isumi Y, Kubo A, Katafuchi T, Kangawa K, Minamino N. Adrenomedullin suppresses interleukin-1beta-induced tumor necrosis factor-alpha production in swiss 3t3 cells. *FEBS Lett*. 1999;463:110-114
9. Shimosawa T, Shibagaki Y, Ishibashi K, Kitamura K, Kangawa K, Kato S, Ando K, Fujita T. Adrenomedullin, an endogenous peptide, counteracts cardiovascular damage. *Circulation*. 2002;105:106-111
10. Nishikimi T, Matsuoka H. Cardiac adrenomedullin: Its role in cardiac hypertrophy and heart failure. *Curr Med Chem Cardiovasc Hematol Agents*. 2005;3:231-242
11. Petrie MC, Hillier C, Morton JJ, McMurray JJ. Adrenomedullin selectively inhibits angiotensin ii-induced aldosterone secretion in humans. *J Hypertens*. 2000;18:61-64
12. Samson WK, Murphy T, Schell DA. A novel vasoactive peptide, adrenomedullin, inhibits pituitary adrenocorticotropin release. *Endocrinology*. 1995;136:2349-2352
13. Shimosawa T, Ogihara T, Matsui H, Asano T, Ando K, Fujita T. Deficiency of adrenomedullin induces insulin resistance by increasing oxidative stress. *Hypertension*. 2003;41:1080-1085
14. Ishimitsu T, Nishikimi T, Saito Y, Kitamura K, Eto T, Kangawa K, Matsuo H, Omae

T, Matsuoka H. Plasma levels of adrenomedullin, a newly identified hypotensive peptide, in patients with hypertension and renal failure. *J Clin Invest*. 1994;94:2158-2161

15. Nishikimi T, Saito Y, Kitamura K, Ishimitsu T, Eto T, Kangawa K, Matsuo H, Omae T, Matsuoka H. Increased plasma levels of adrenomedullin in patients with heart failure. *J Am Coll Cardiol*. 1995;26:1424-1431
16. Kronenberg F. Emerging risk factors and markers of chronic kidney disease progression. *Nat Rev Nephrol*. 2009;5:677-689
17. Shindo T, Kurihara Y, Nishimatsu H, Moriyama N, Kakoki M, Wang Y, Imai Y, Ebihara A, Kuwaki T, Ju KH, Minamino N, Kangawa K, Ishikawa T, Fukuda M, Akimoto Y, Kawakami H, Imai T, Morita H, Yazaki Y, Nagai R, Hirata Y, Kurihara H. Vascular abnormalities and elevated blood pressure in mice lacking adrenomedullin gene. *Circulation*. 2001;104:1964-1971
18. Nagaya N, Mori H, Murakami S, Kangawa K, Kitamura S. Adrenomedullin: Angiogenesis and gene therapy. *Am J Physiol Regul Integr Comp Physiol*. 2005;288:R1432-1437
19. Iwase T, Nagaya N, Fujii T, Itoh T, Ishibashi-Ueda H, Yamagishi M, Miyatake K, Matsumoto T, Kitamura S, Kangawa K. Adrenomedullin enhances angiogenic potency of bone marrow transplantation in a rat model of hindlimb ischemia. *Circulation*. 2005;111:356-362
20. Hanabusa K, Nagaya N, Iwase T, Itoh T, Murakami S, Shimizu Y, Taki W, Miyatake K, Kangawa K. Adrenomedullin enhances therapeutic potency of mesenchymal stem cells after experimental stroke in rats. *Stroke*. 2005;36:853-858
21. Iimuro S, Shindo T, Moriyama N, Amaki T, Niu P, Takeda N, Iwata H, Zhang Y, Ebihara A, Nagai R. Angiogenic effects of adrenomedullin in ischemia and tumor growth. *Circ Res*. 2004;95:415-423
22. Maki T, Ihara M, Fujita Y, Nambu T, Miyashita K, Yamada M, Washida K, Nishio K, Ito H, Harada H, Yokoi H, Arai H, Itoh H, Nakao K, Takahashi R, Tomimoto H. Angiogenic and vasoprotective effects of adrenomedullin on prevention of cognitive decline after chronic cerebral hypoperfusion in mice. *Stroke*. 2011;42:1122-1128
23. McLatchie LM, Fraser NJ, Main MJ, Wise A, Brown J, Thompson N, Solari R, Lee MG, Foord SM. Ramps regulate the transport and ligand specificity of the calcitonin-receptor-like receptor. *Nature*. 1998;393:333-339
24. Parameswaran N, Spielman WS. Ramps: The past, present and future. *Trends Biochem Sci*. 2006;31:631-638

25. Ichikawa-Shindo Y, Sakurai T, Kamiyoshi A, Kawate H, Iinuma N, Yoshizawa T, Koyama T, Fukuchi J, Iimuro S, Moriyama N, Kawakami H, Murata T, Kangawa K, Nagai R, Shindo T. The gpcr modulator protein ramp2 is essential for angiogenesis and vascular integrity. *J Clin Invest*. 2008;118:29-39
26. Fernandez AP, Serrano J, Tessarollo L, Cuttitta F, Martinez A. Lack of adrenomedullin in the mouse brain results in behavioral changes, anxiety, and lower survival under stress conditions. *Proc Natl Acad Sci U S A*. 2008;105:12581-12586
27. Minamino T, Yoshida T, Tateno K, Miyauchi H, Zou Y, Toko H, Komuro I. Ras induces vascular smooth muscle cell senescence and inflammation in human atherosclerosis. *Circulation*. 2003;108:2264-2269
28. Miyauchi H, Minamino T, Tateno K, Kunieda T, Toko H, Komuro I. Akt negatively regulates the in vitro lifespan of human endothelial cells via a p53/p21-dependent pathway. *Embo J*. 2004;23:212-220
29. Chen Q, Ames BN. Senescence-like growth arrest induced by hydrogen peroxide in human diploid fibroblast f65 cells. *Proc Natl Acad Sci U S A*. 1994;91:4130-4134
30. Prasain N, Stevens T. The actin cytoskeleton in endothelial cell phenotypes. *Microvasc Res*. 2009;77:53-63
31. Fritz-Six KL, Dunworth WP, Li M, Caron KM. Adrenomedullin signaling is necessary for murine lymphatic vascular development. *J Clin Invest*. 2008;118:40-50
32. Takahashi H, Watanabe TX, Nishimura M, Nakanishi T, Sakamoto M, Yoshimura M, Komiyama Y, Masuda M, Murakami T. Centrally induced vasopressor and sympathetic responses to a novel endogenous peptide, adrenomedullin, in anesthetized rats. *Am J Hypertens*. 1994;7:478-482
33. Minamino T, Komuro I. Vascular aging: Insights from studies on cellular senescence, stem cell aging, and progeroid syndromes. *Nat Clin Pract Cardiovasc Med*. 2008;5:637-648
34. Minamino T, Komuro I. Vascular cell senescence: Contribution to atherosclerosis. *Circ Res*. 2007;100:15-26
35. Longo VD, Finch CE. Evolutionary medicine: From dwarf model systems to healthy centenarians? *Science*. 2003;299:1342-1346
36. Iinuma N, Sakurai T, Kamiyoshi A, Ichikawa-Shindo Y, Arai T, Yoshizawa T, Koyama T, Uetake R, Kawate H, Muto S, Tagawa Y, Miyagawa S, Shindo T. Adrenomedullin in sinusoidal endothelial cells play protective roles against cold injury of liver. *Peptides*. 2010;31:865-871
37. Temmesfeld-Wollbruck B, Hocke AC, Suttorp N, Hippenstiel S. Adrenomedullin and

endothelial barrier function. *Thromb Haemost*. 2007;98:944-951

38. Fukuhara S, Sakurai A, Sano H, Yamagishi A, Somekawa S, Takakura N, Saito Y, Kangawa K, Mochizuki N. Cyclic amp potentiates vascular endothelial cadherin-mediated cell-cell contact to enhance endothelial barrier function through an epac-rap1 signaling pathway. *Mol Cell Biol*. 2005;25:136-146
39. Aslam M, Gunduz D, Schuler D, Li L, Sharifpanah F, Sedding D, Piper HM, Noll T. Intermedin induces loss of coronary microvascular endothelial barrier via derangement of actin cytoskeleton: Role of rhoa and rac1. *Cardiovasc Res*. 2011;92:276-286
40. Sano M, Kuroi N, Nakayama T, Sato N, Izumi Y, Soma M, Kokubun S. Association study of calcitonin-receptor-like receptor gene in essential hypertension. *Am J Hypertens*. 2005;18:403-408
41. Nakazato T, Nakayama T, Naganuma T, Sato N, Fu Z, Wang Z, Soma M, Sugama K, Hinohara S, Doba N. Haplotype-based case-control study of receptor (calcitonin) activity-modifying protein-1 gene in cerebral infarction. *J Hum Hypertens*. 2010;24:351-358
42. Bailey RJ, Bradley JW, Poyner DR, Rathbone DL, Hay DL. Functional characterization of two human receptor activity-modifying protein 3 variants. *Peptides*. 2010;31:579-584

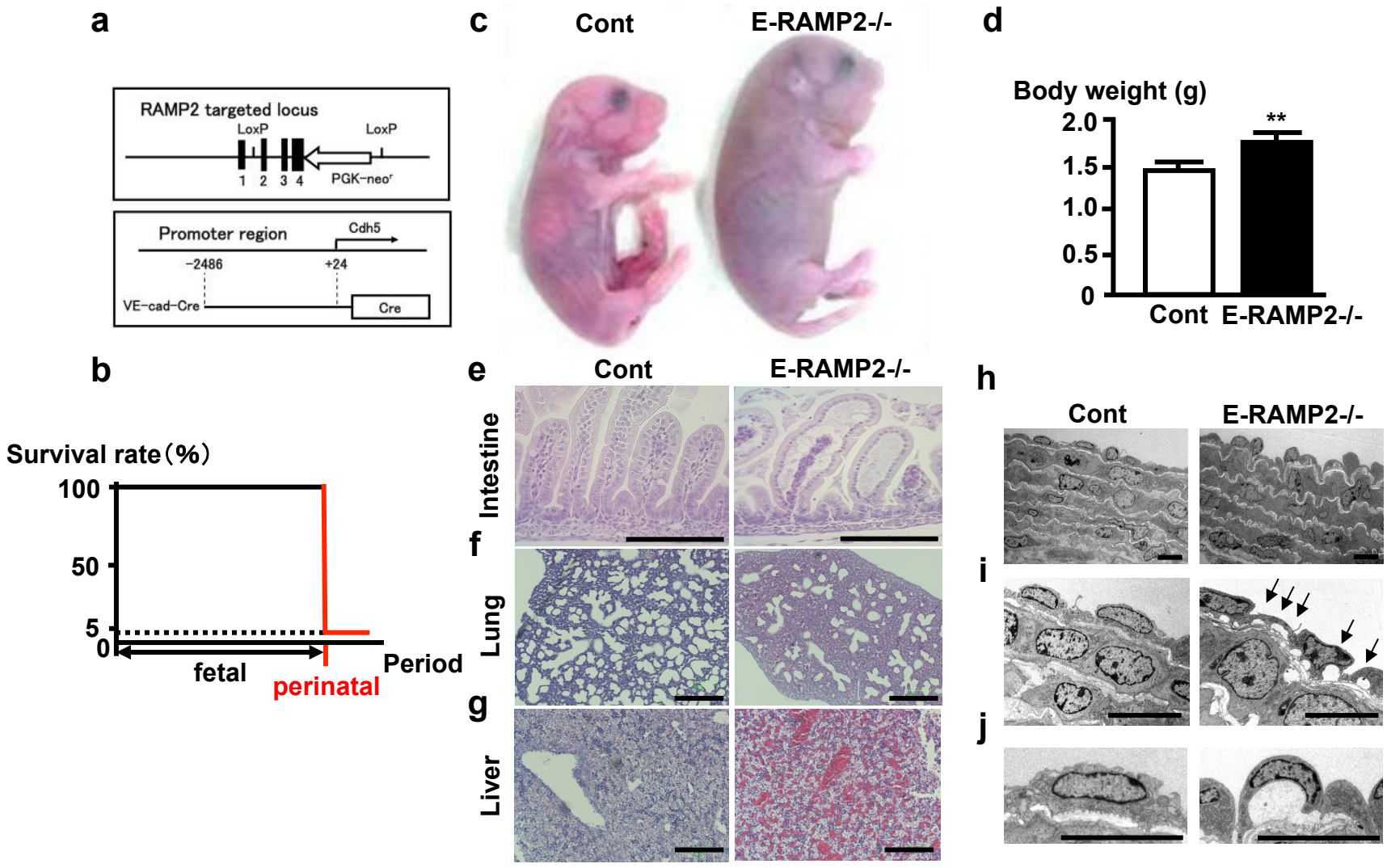
a
RAMP2 targeted locus
LoxP
LoxP
1 2 3 4
PGK-neo
Promoter region
Cdh5
-2486
+24
VE-cad-Cre
Cre
b
Survival rate (%)
100
50
5
0
fetal
perinatal
Period
c
Cont
E-RAMP2-/-
d
Body weight (g)
2.0
1.5
1.0
0.5
0
**
Cont
E-RAMP2-/-
e
Cont
E-RAMP2-/-
Intestine
f
Lung
g
Liver
h
Cont
E-RAMP2-/-
i
j

Fig.1

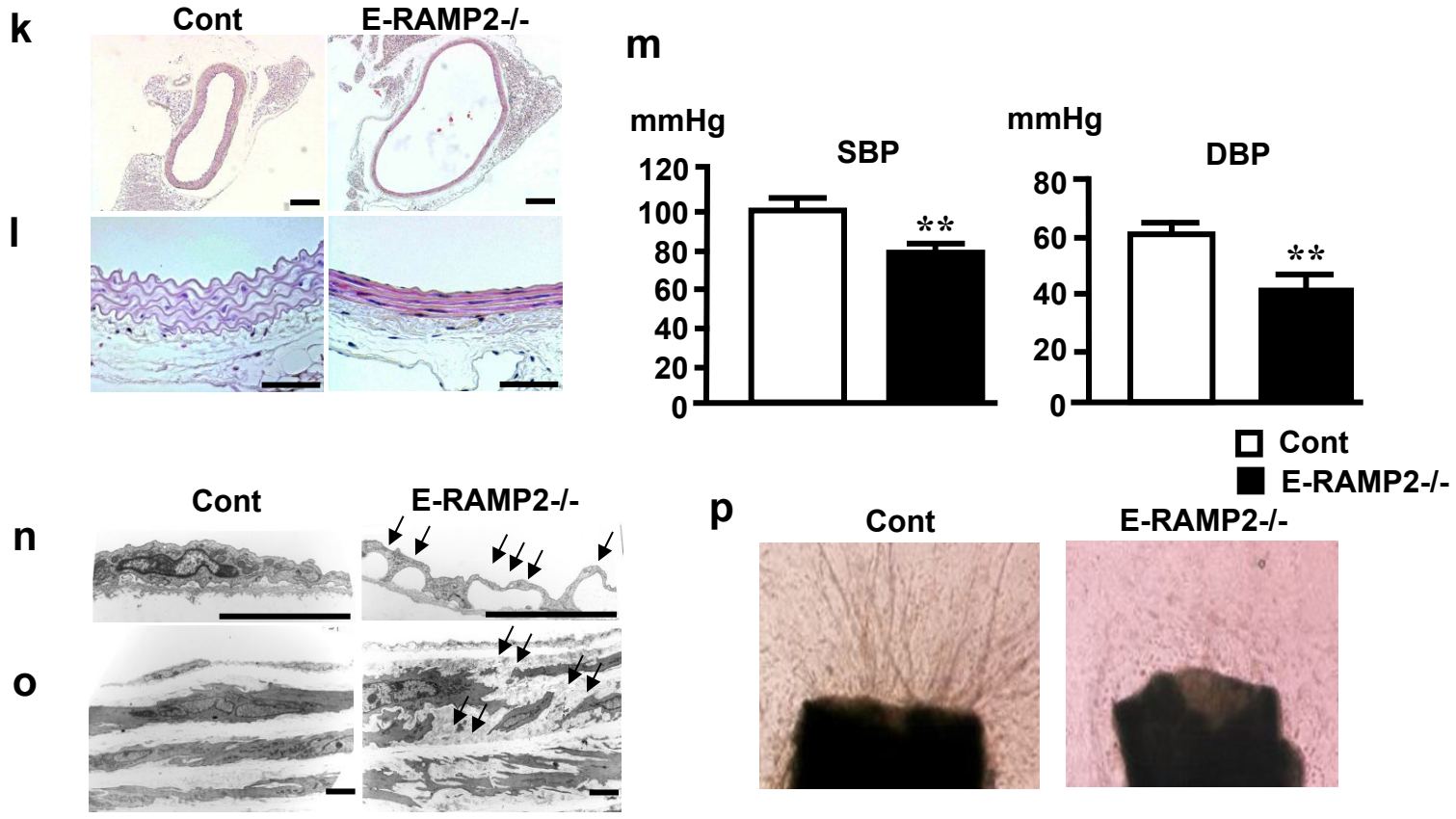
k
Cont
E-RAMP2-/-
l
m
mmHg
SBP
120
100
80
60
40
20
0
**
mmHg
DBP
80
60
40
20
0
**
Cont
E-RAMP2-/-
n
Cont
E-RAMP2-/-
o
p
Cont
E-RAMP2-/-

Fig.1

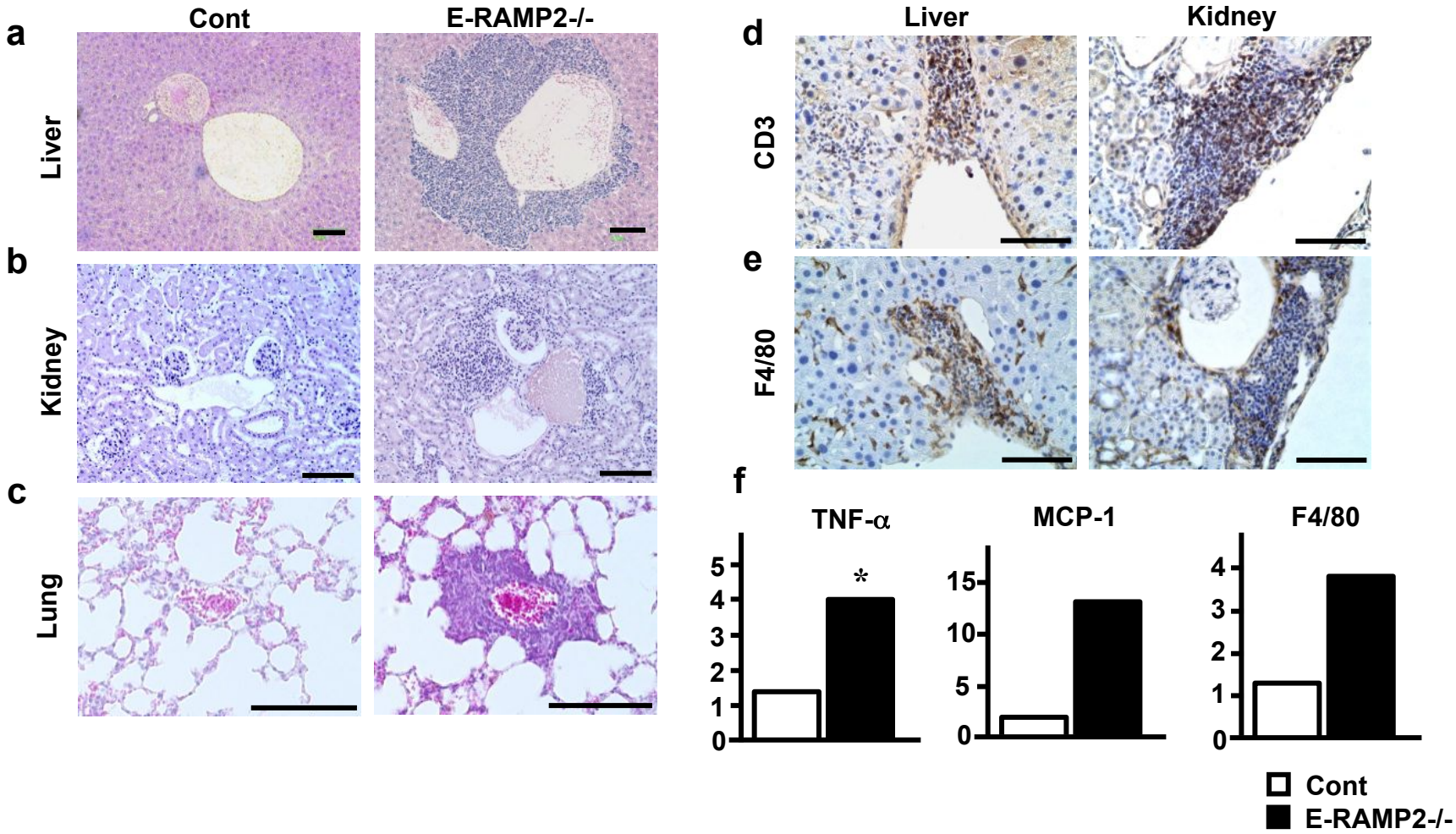
a
Cont
E-RAMP2-/-
Liver
b
Kidney
c
Lung
d
Liver
Kidney
CD3
e
F4/80
f
TNF-α
MCP-1
F4/80
*
Cont
E-RAMP2-/-

Fig.2

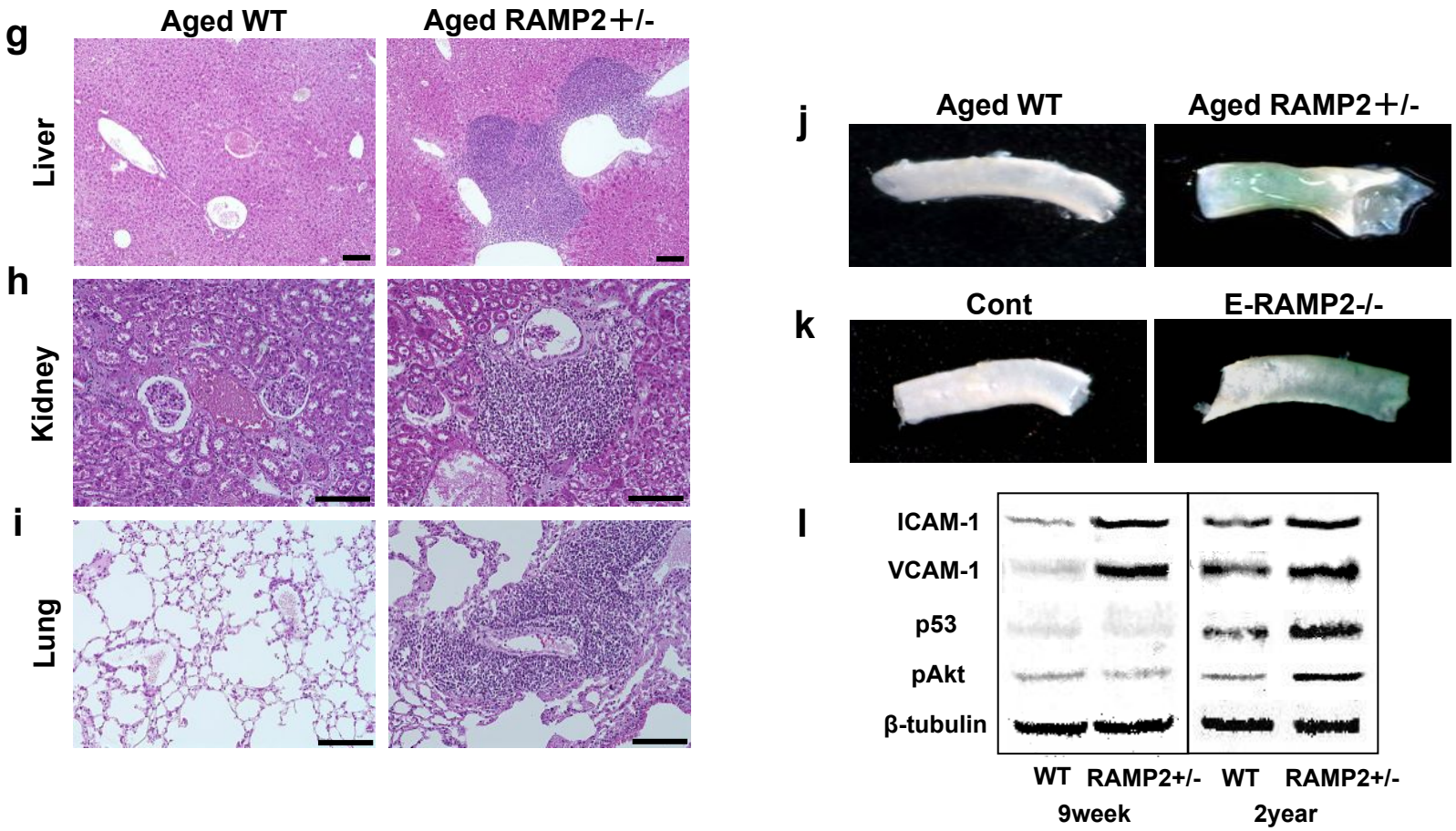
g
Aged WT
Aged RAMP2+/-
Liver
h
Kidney
i
Lung
j
Aged WT
Aged RAMP2+/-
k
Cont
E-RAMP2-/-
l
ICAM-1
VCAM-1
p53
pAkt
β-tubulin
WT
RAMP2+/-
WT
RAMP2+/-
9week
2year

Fig.2

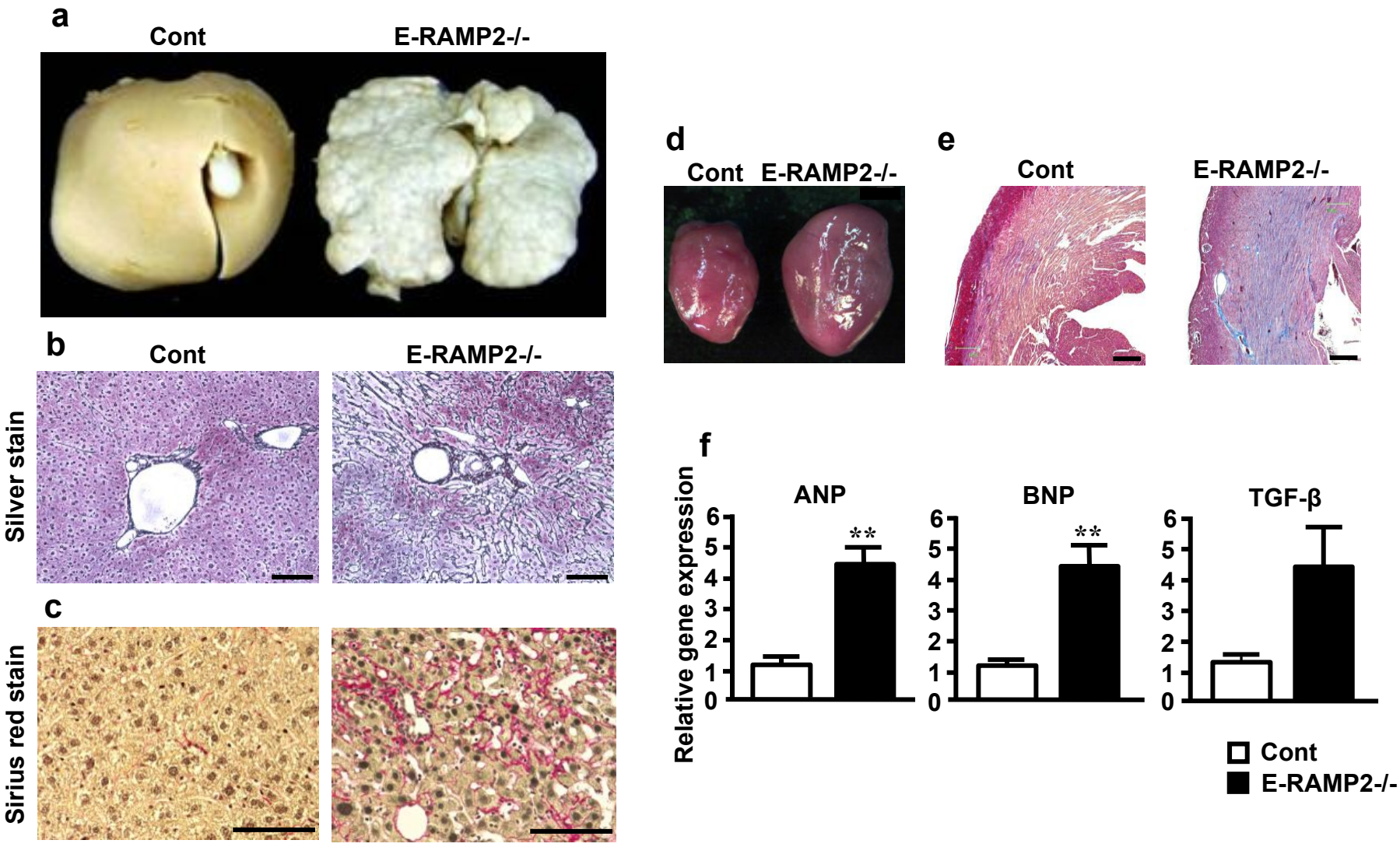
a
Cont
E-RAMP2-/-
b
Cont
E-RAMP2-/-
Silver stain
c
Sirius red stain
d
Cont
E-RAMP2-/-
e
Cont
E-RAMP2-/-
f
ANP
BNP
TGF-β
Relative gene expression
0
1
2
3
4
5
6
**
**
Cont
E-RAMP2-/-

Fig.3

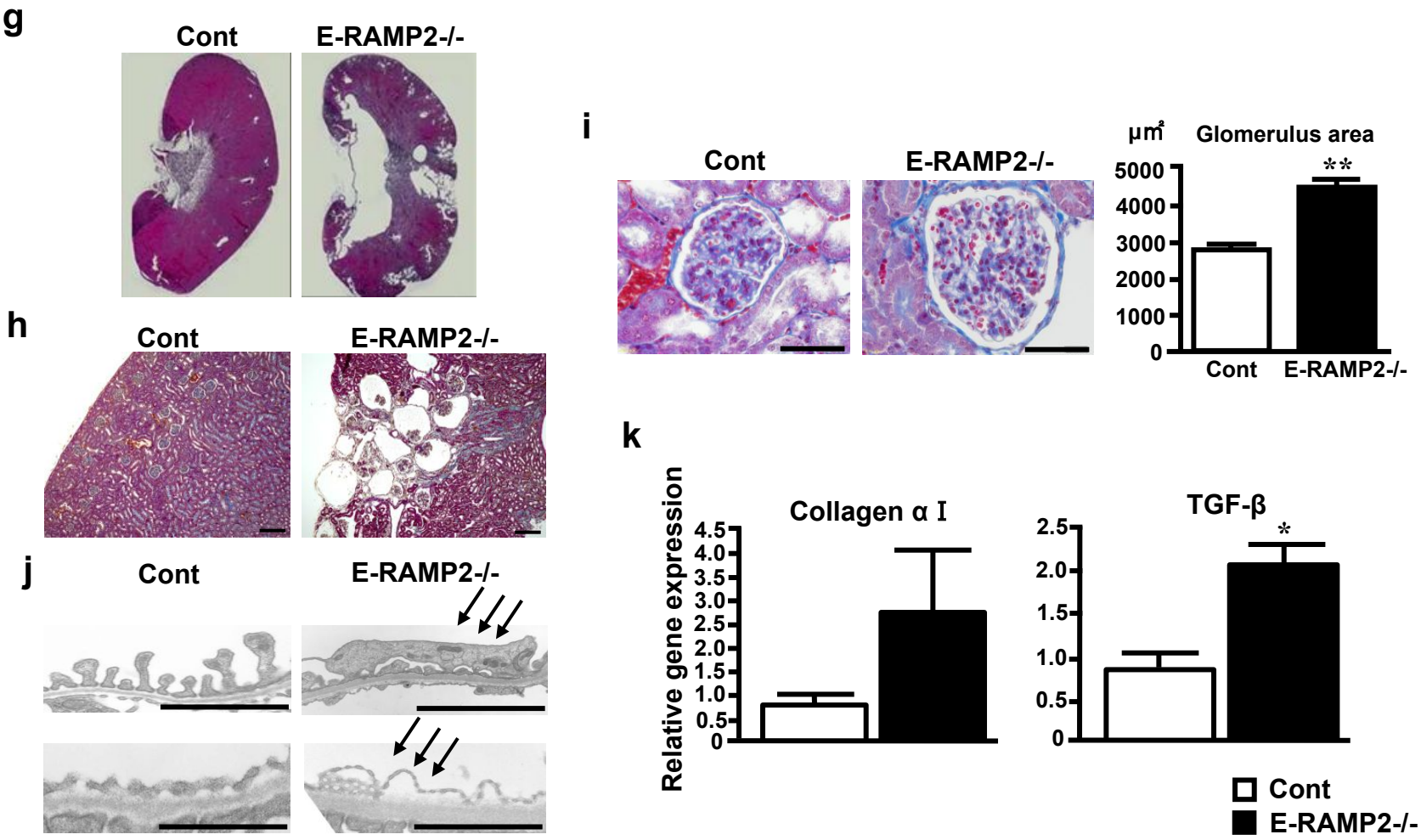
g
Cont
E-RAMP2-/-
h
Cont
E-RAMP2-/-
j
Cont
E-RAMP2-/-
i
Cont
E-RAMP2-/-
μm²
Glomerulus area
**
5000
4000
3000
2000
1000
0
Cont
E-RAMP2-/-
k
Relative gene expression
Collagen α I
4.5
4.0
3.5
3.0
2.5
2.0
1.5
1.0
0.5
0
TGF-β
*
2.5
2.0
1.5
1.0
0.5
0
Cont
E-RAMP2-/-

Fig.3

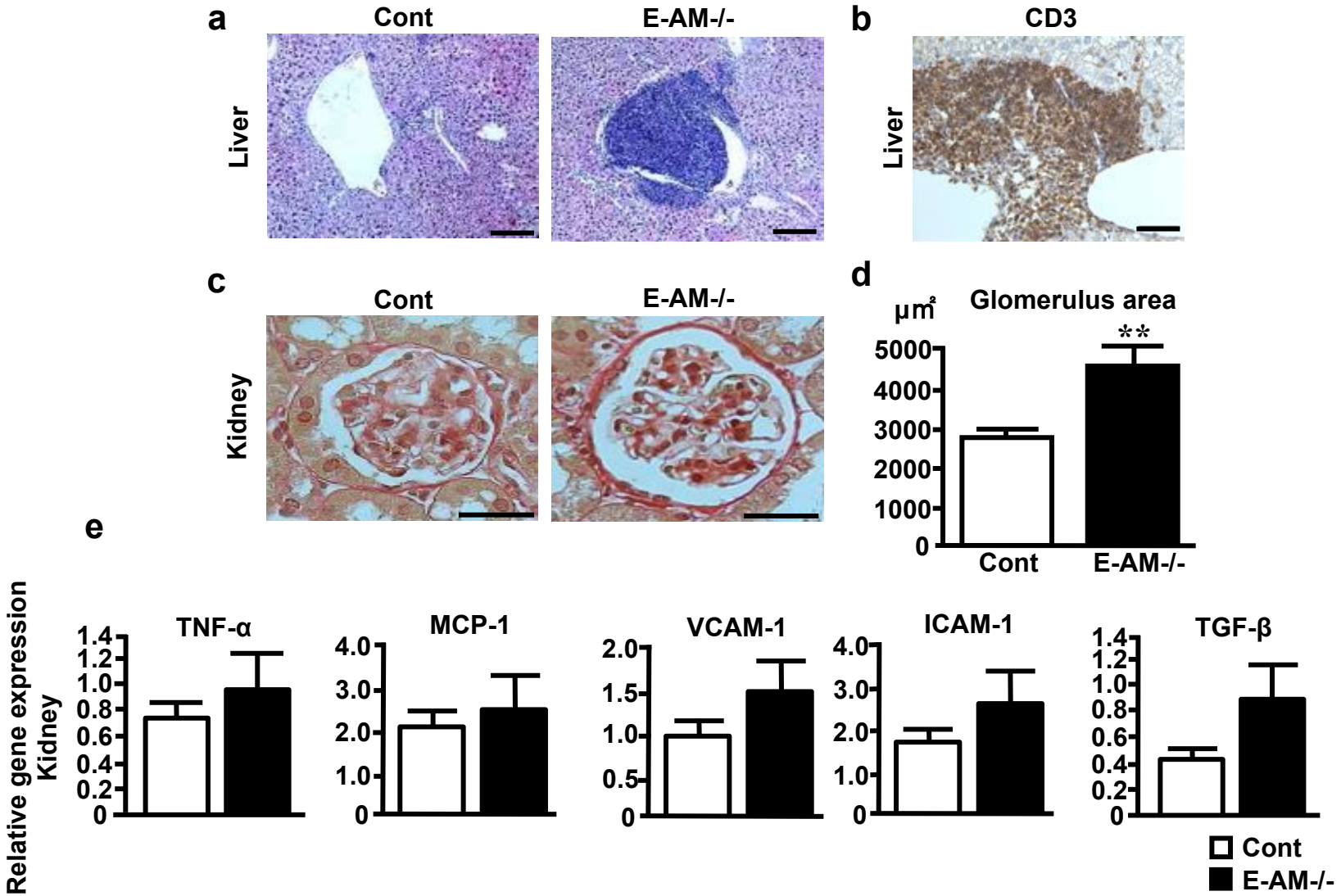
a
Cont
E-AM-/-
Liver
b
CD3
Liver
c
Cont
E-AM-/-
Kidney
d
μm²
Glomerulus area
**
5000
4000
3000
2000
1000
0
Cont
E-AM-/-
e
Relative gene expression
Kidney
TNF-α
MCP-1
VCAM-1
ICAM-1
TGF-β
Cont
E-AM-/-

Fig.4

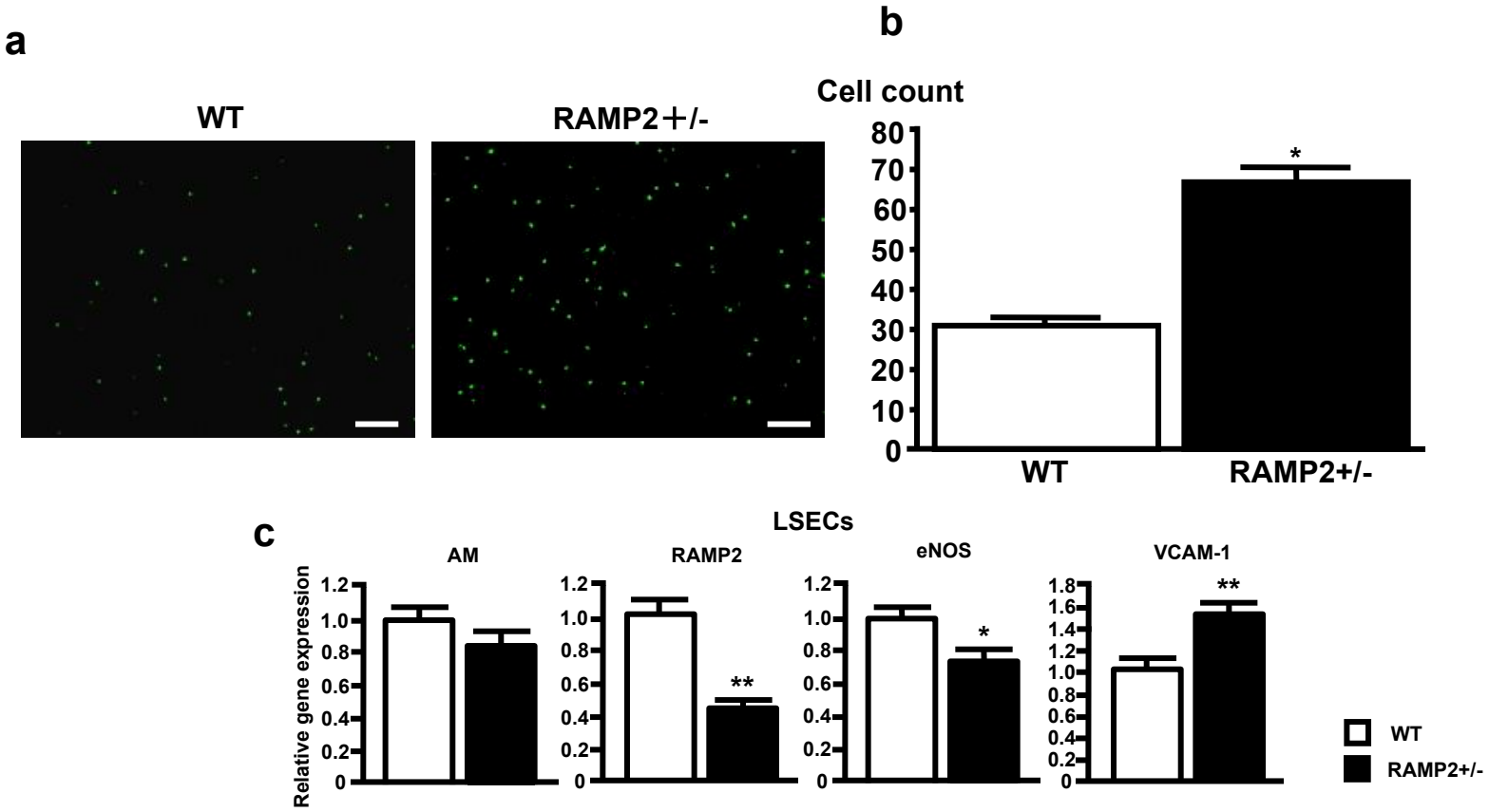
a
WT
RAMP2+/-
b
Cell count
80
70
60
50
40
30
20
10
0
*
WT
RAMP2+/-
c
LSECs
AM
RAMP2
eNOS
VCAM-1
Relative gene expression
1.2
1.0
0.8
0.6
0.4
0.2
0
**
*
1.8
1.6
1.4
**
WT
RAMP2+/-

Fig.5

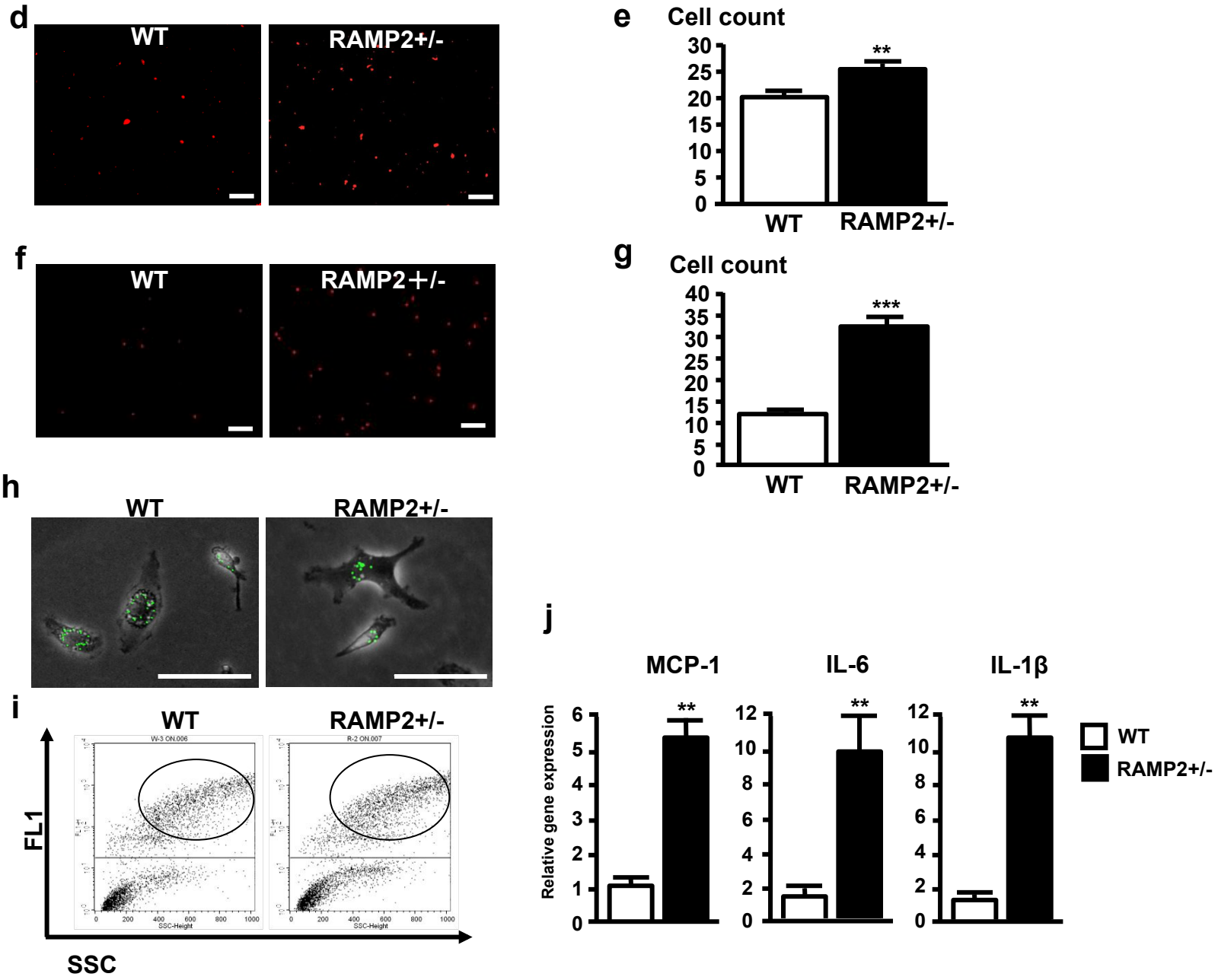
d
WT
RAMP2+/-
e
Cell count
30
25
20
15
10
5
0
**
WT
RAMP2+/-
f
WT
RAMP2+/-
g
Cell count
40
35
30
25
20
15
10
5
0
***
WT
RAMP2+/-
h
WT
RAMP2+/-
i
WT
RAMP2+/-
FL1
SSC
W-3 ON.006
R-2 ON.007
SSC-Height
j
MCP-1
IL-6
IL-1β
Relative gene expression
**
WT
RAMP2+/-

Fig.5

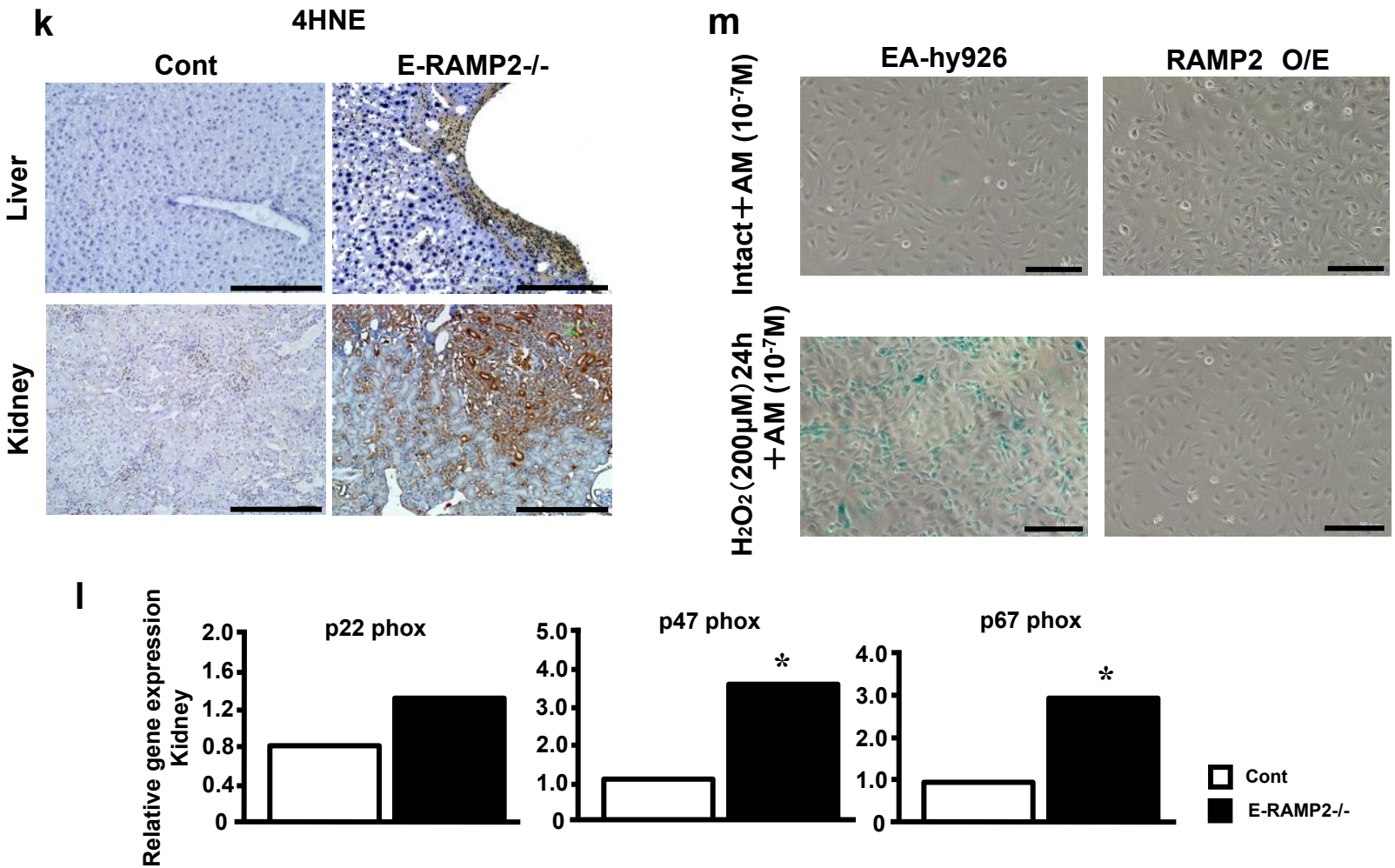
k
4HNE
Cont
E-RAMP2-/-
Liver
Kidney
m
EA-hy926
RAMP2 O/E
Intact+AM (10-7M)
H2O2(200μM)24h +AM (10-7M)
l
Relative gene expression Kidney
p22 phox
p47 phox
p67 phox
2.0
1.6
1.2
0.8
0.4
0
5.0
4.0
3.0
2.0
1.0
0
4.0
3.0
2.0
1.0
0
*
*
Cont
E-RAMP2-/-

Fig.5

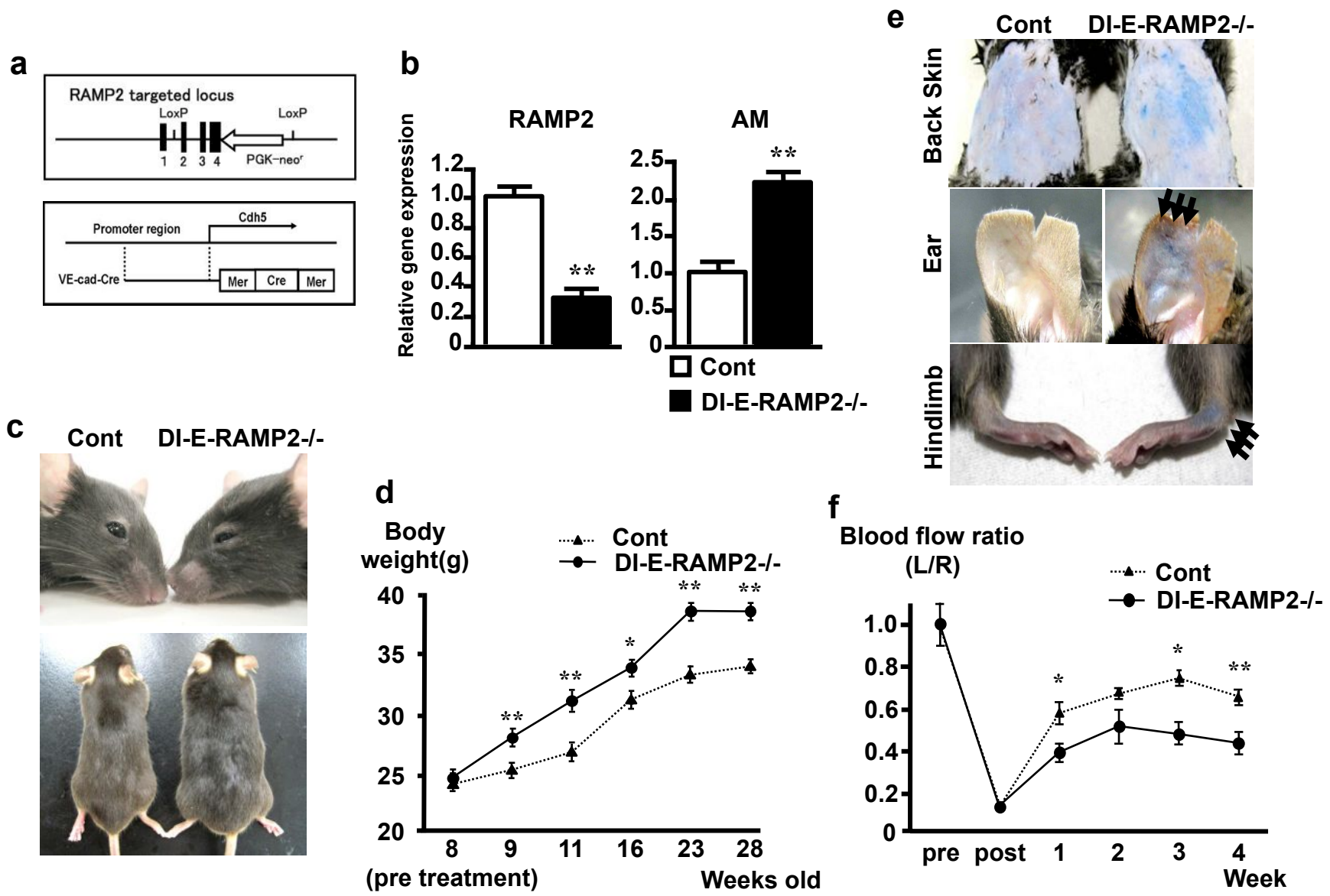
a
RAMP2 targeted locus
LoxP
LoxP
1 2 3 4
PGK-neo^r
Promoter region
Cdh5
VE-cad-Cre
Mer
Cre
Mer
b
RAMP2
AM
Relative gene expression
1.2
1.0
0.8
0.6
0.4
0.2
0
**
2.5
2.0
1.5
1.0
0.5
0
**
Cont
DI-E-RAMP2-/-
c
Cont
DI-E-RAMP2-/-
d
Body weight(g)
Cont
DI-E-RAMP2-/-
40
35
30
25
20
**
**
**
*
8
9
11
16
23
28
(pre treatment)
Weeks old
e
Cont
DI-E-RAMP2-/-
Back Skin
Ear
Hindlimb
f
Blood flow ratio (L/R)
Cont
DI-E-RAMP2-/-
1.0
0.8
0.6
0.4
0.2
0
*
*
**
pre
post
1
2
3
4
Week

Fig.6

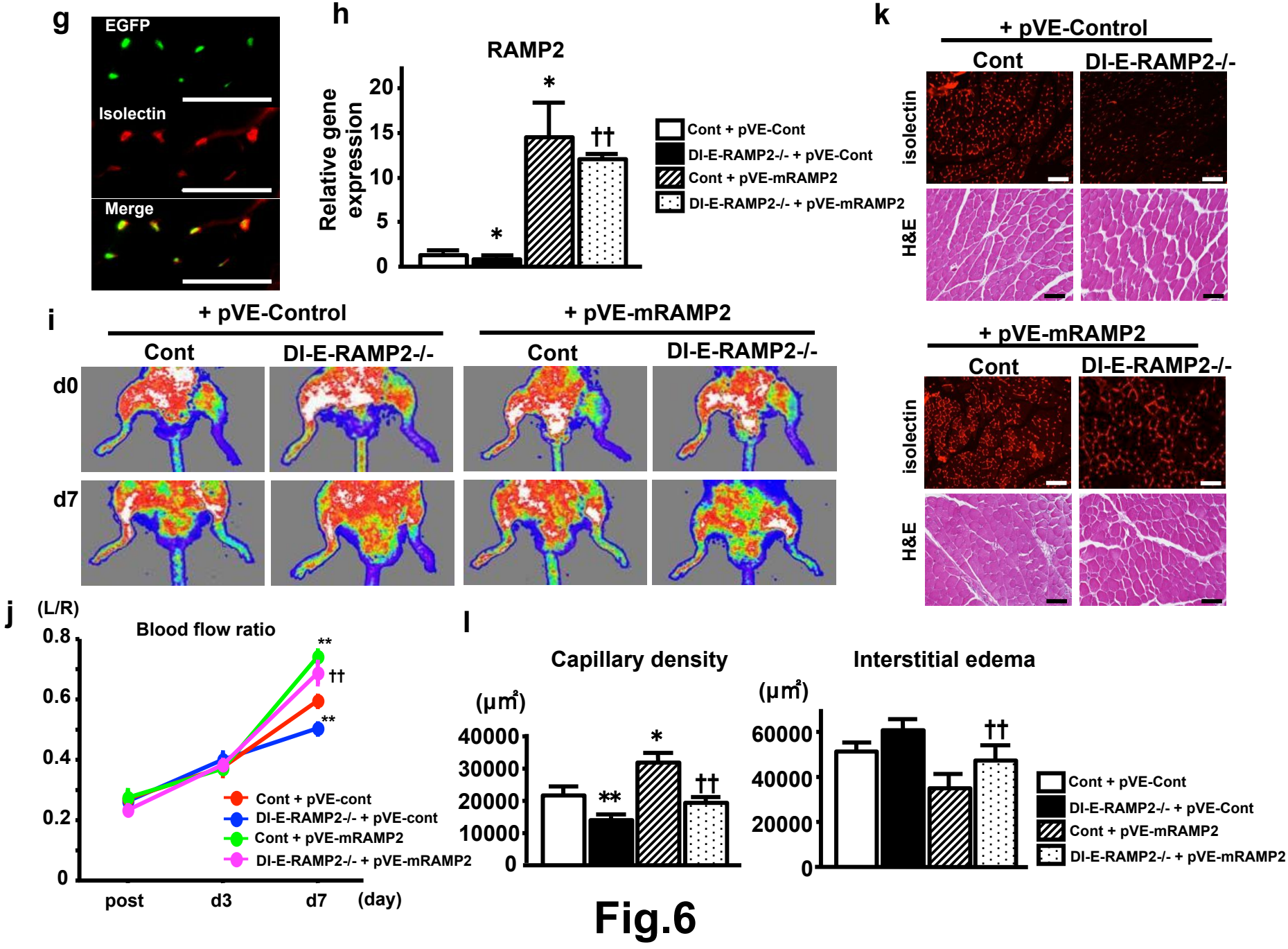
g
EGFP
Isolectin
Merge
h
RAMP2
Relative gene expression
20
15
10
5
0
*
*
††
Cont + pVE-Cont
DI-E-RAMP2-/- + pVE-Cont
Cont + pVE-mRAMP2
DI-E-RAMP2-/- + pVE-mRAMP2
k
+ pVE-Control
Cont
DI-E-RAMP2-/-
isolectin
H&E
+ pVE-mRAMP2
Cont
DI-E-RAMP2-/-
isolectin
H&E
i
+ pVE-Control
+ pVE-mRAMP2
Cont
DI-E-RAMP2-/-
Cont
DI-E-RAMP2-/-
d0
d7
j
(L/R)
Blood flow ratio
0.8
0.6
0.4
0.2
0
**
††
**
Cont + pVE-cont
DI-E-RAMP2-/- + pVE-cont
Cont + pVE-mRAMP2
DI-E-RAMP2-/- + pVE-mRAMP2
post
d3
d7
(day)
l
Capillary density
(μm²)
40000
30000
20000
10000
0
**
*
††
Interstitial edema
(μm²)
60000
40000
20000
0
††
Cont + pVE-Cont
DI-E-RAMP2-/- + pVE-Cont
Cont + pVE-mRAMP2
DI-E-RAMP2-/- + pVE-mRAMP2

Fig.6

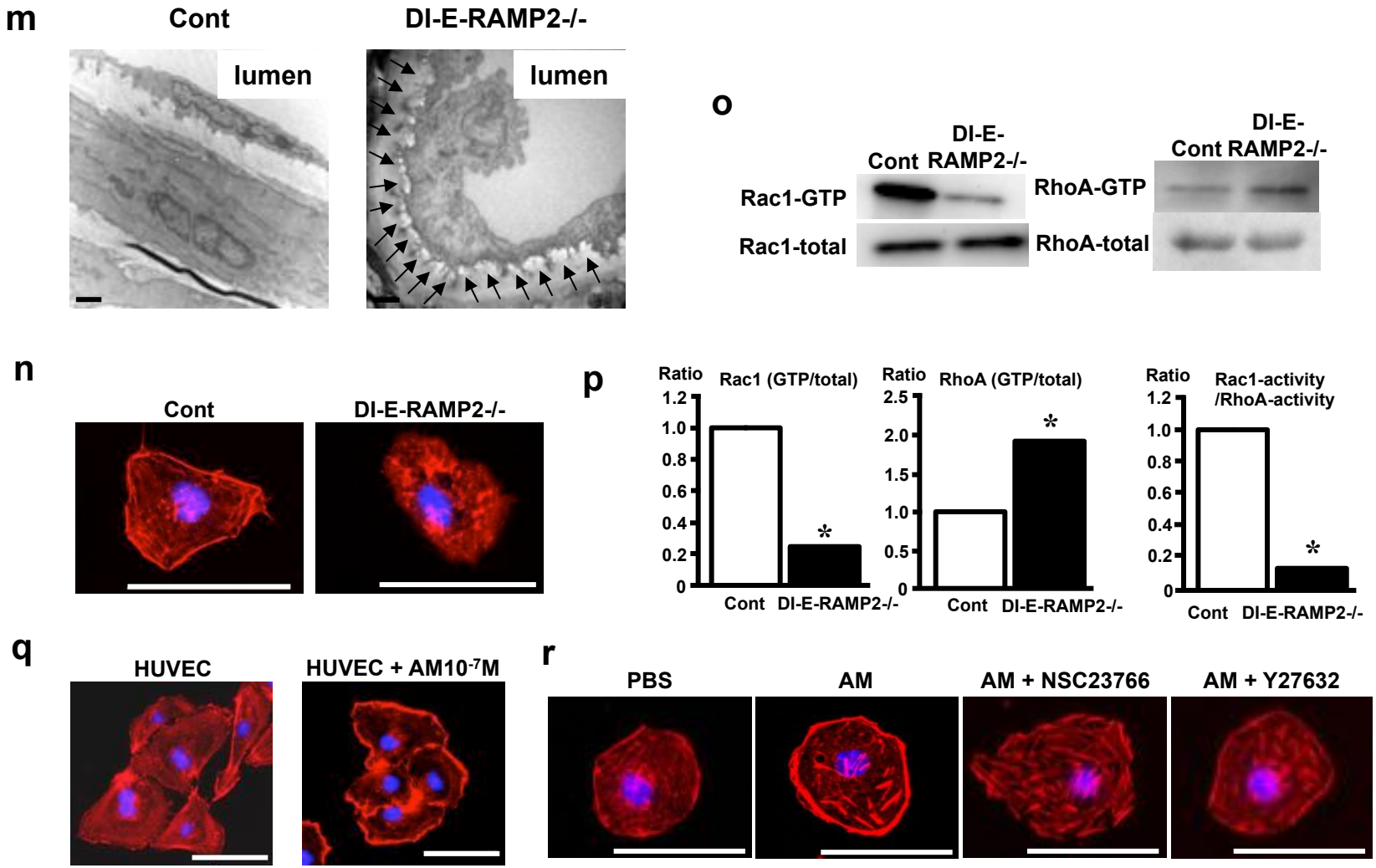
m
Cont
DI-E-RAMP2-/-
lumen
lumen
o
Cont
DI-E-RAMP2-/-
Rac1-GTP
Rac1-total
RhoA-GTP
RhoA-total
Cont
DI-E-RAMP2-/-
n
Cont
DI-E-RAMP2-/-
p
Ratio
Rac1 (GTP/total)
1.2
1.0
0.8
0.6
0.4
0.2
0
*
Cont
DI-E-RAMP2-/-
Ratio
RhoA (GTP/total)
2.5
2.0
1.5
1.0
0.5
0
*
Cont
DI-E-RAMP2-/-
Ratio
Rac1-activity
/RhoA-activity
1.2
1.0
0.8
0.6
0.4
0.2
0
*
Cont
DI-E-RAMP2-/-
q
HUVEC
HUVEC + AM10-7M
r
PBS
AM
AM + NSC23766
AM + Y27632

Fig.6

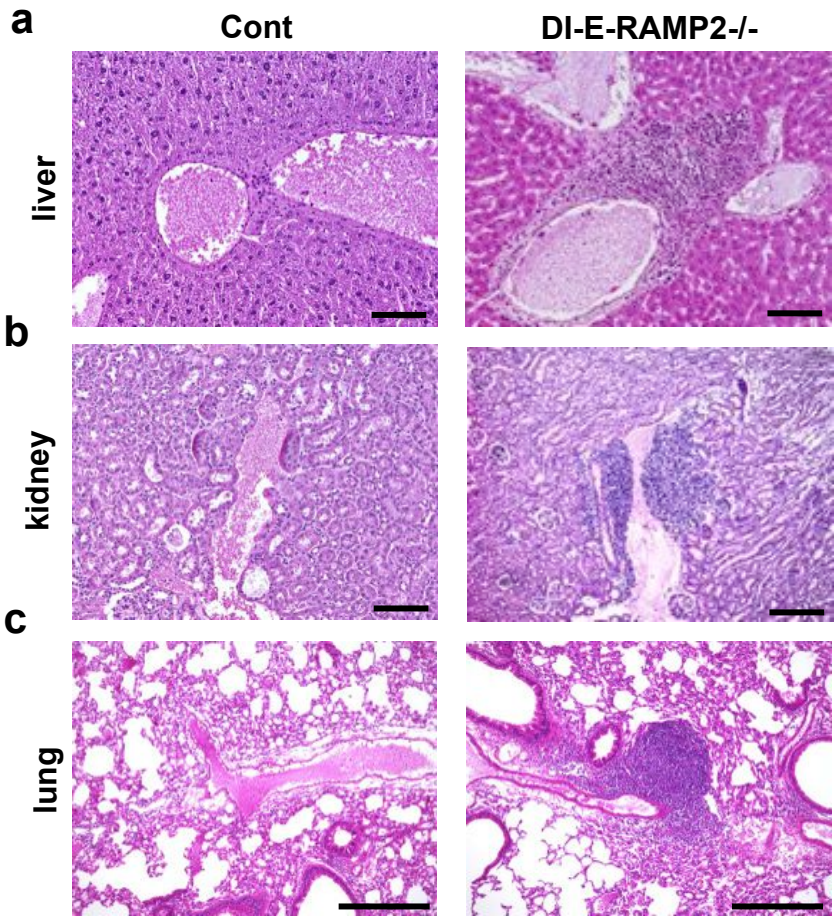

Fig.7

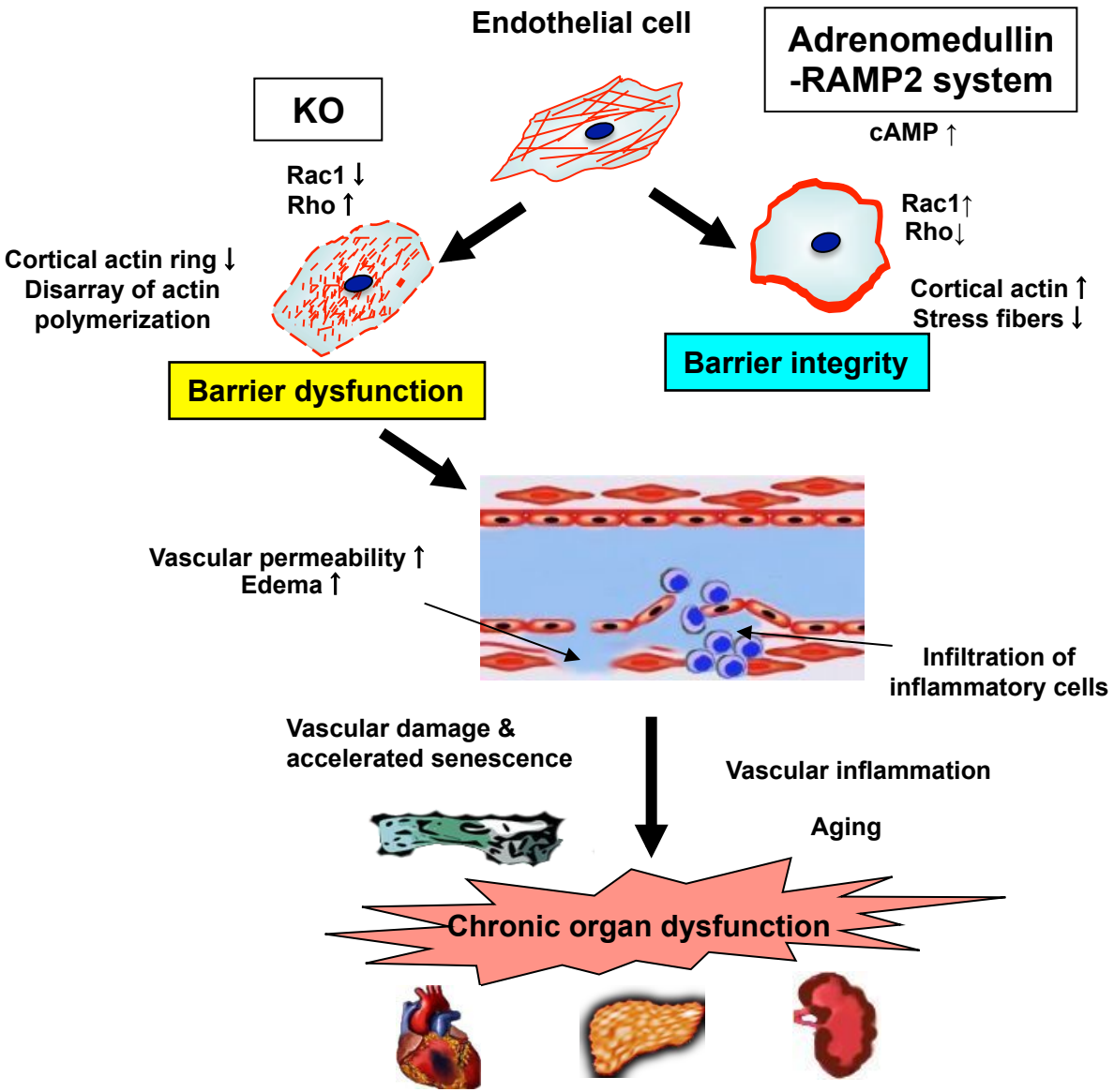
Endothelial cell
Adrenomedullin
-RAMP2 system
cAMP ↑
KO
Rac1 ↓
Rho ↑
Cortical actin ring ↓
Disarray of actin
polymerization
Rac1↑
Rho↓
Cortical actin ↑
Stress fibers ↓
Barrier dysfunction
Barrier integrity
Vascular permeability ↑
Edema ↑
Infiltration of
inflammatory cells
Vascular damage &
accelerated senescence
Vascular inflammation
Aging
Chronic organ dysfunction

Fig.8